Copyright Warning & Restrictions

The copyright law of the United States (Title 17, United States Code) governs the making of photocopies or other reproductions of copyrighted material.

Under certain conditions specified in the law, libraries and archives are authorized to furnish a photocopy or other reproduction. One of these specified conditions is that the photocopy or reproduction is not to be "used for any purpose other than private study, scholarship, or research." If a, user makes a request for, or later uses, a photocopy or reproduction for purposes in excess of "fair use" that user may be liable for copyright infringement,

This institution reserves the right to refuse to accept a copying order if, in its judgment, fulfillment of the order would involve violation of copyright law.

Please Note: The author retains the copyright while the New Jersey Institute of Technology reserves the right to distribute this thesis or dissertation

Printing note: If you do not wish to print this page, then select "Pages from: first page # to: last page #" on the print dialog screen

PREPARATION AND MAGNETIC PROPERTIES OF RARE EARTH GARNETS AND APATITES

BY

ROSTAM MONDEGARIAN

A DISSERTATION

PRESENTED IN PARTIAL FULFILLMENT OF

THE REQUIREMENTS FOR THE DEGREE

OF

DOCTOR OF ENGINEERING SCIENCE IN CHEMICAL ENGINEERING

AT

NEW JERSEY INSTITUTE OF TECHNOLOGY

Newark, New Jersey
1976

APPROVAL OF DISSERTATION

PREPARATION AND MAGNETIC PROPERTIES OF RARE EARTH GARNETS AND APATITES

BY

ROSTAM MONDEGARIAN

FOR

DEPARTMENT OF CHEMICAL ENGINEERING AND CHEMISTRY

BY

FACULTY COMMITTEE

APPROVED:

Lawrence Suchow, Chairman

Howard S. Kimmel

Don G. Lambert

Ching-Hong Huang

Robert E. McMillan

NEWARK, NEW JERSEY
MAY, 1976

ACKNOWLEDGMENT

The author wishes to express his appreciation to Dr. Lawrence Suchow, for his guidance and kind supervision throughout this work and through the years of graduate study.

Dr. Howard S. Kimmel, Dr. Ching-Rong Huang and Dr. Robert McMillan are each thanked for serving on the advisory committee.

The author also wishes to thank R. C. Sherwood and G. Hull of Bell Telephone Laboratories, Murray Hill, New Jersey for their help in magnetic measurements.

Finally, I find it difficult to adequately express my appreciation to my wife, Georgene, who encouraged me when I needed it the most.

ABSTRACT

It has been found possible to prepare garnets with magnetic trivalent rare earth ions filling all or most dodecahedral sites while nonmagnetic Sc^{3+} ions fill all octahedral sites and magnetic Fe^{3+} ions fill all or most tetrahedral sites. Phase-pure garnets found include $\{RE_{3-y}Sc_y\}[Sc_2](Fe_3)O_{12}$, where RE is Sm, Eu, Gd, Tb or Dy and y can be zero with Sm and Eu; $\{Nd_3\}[Sc_2](Fe_zGa_{3-z})O_{12}$; and other Nd-Sc-Fe garnets of the type $\{Nd_{3-(w+y)}M_wSc_y\}[Sc_2](Fe_3)O_{12}$, where M is Gd, Y, and Lu.

Compositions chosen for magnetic studies were those with maximum allowable concentrations of magnetic ions on the dodecahedral and tetrahedral sites. In each case, dependence of magnetization on temperature was measured between room temperature and that of liquid helium. Measurements were also made at liquid helium temperature of the dependence of magnetization on applied field with values up to 60 kOe. Ordering ascribed to ferrimagnetism and perhaps also antiferromagentism has been observed. Saturation has not been obtained with the maximum field applied, apparently because of canting of magnetic ion moments when the octahedral sites contain only diamagnetic ions.

Calculations of structure factors have confirmed the structural formulae $\{Nd_{2.7}Yb_{0.3}\}[Yb_2](Ga_3)O_{12}$ and $Pr_3[Lu_2](Ga_3)O_{12}$; that is, rare earths fill all dodecahedral and octahedral sites.

Oxyapatites are typified by $Ca_4La(PO_4)_3O$ and $Ca\ Y_4(SiO_4)_3O$ (or $A_5B_3O_{13}$) and $Ca_5(PO_4)_3O_{0.5}\square_{0.5}$ (or $A_5B_3O_{12.5}$), where $\square$

represents a vacancy. Such oxyapatites have in each formula unit as written here three A cations with one type of coordination and the other two another type, three tetrahedral B cations, and 13 or 12.5 oxide ions. These ionic ratios (3:2:3:13-12.5) are therefore very close to those found in garnets (3:2:3:12). Attempts were made to prepare rare earth-iron apatites in order to seek magnetic interactions like those in garnets, but apatites did not form.

TABLE OF CONTENTS

TABLE OF CONTENTS (Continued)

LIST OF FIGURES

LIST OF FIGURES (Continued)

LIST OF TABLES

LIST OF TABLES (Continued)

LIST OF TABLES (Continued)

I. INTRODUCTION

I.1 Problem Studied

The work reported herein has consisted of miscellaneous studies of new rare earth compounds and it has been oriented toward three subjects:

1. The confirmation by structure factor calculations of filling by rare earths of two crystallographic sites of the garnet structure.
2. Preparation of new rare earth garnets and study of their magnetic properties.
3. Attempts to prepare new rare earth apatites.

I.2 Classification of Magnetic Properties

Considerable emphasis and importance has been placed upon the determination of magnetic properties of transition metal and rare earth compounds. Such studies have contributed much to characterization of these compounds. Before considering just how this has been possible it will be of value to examine the origins and types of magnetic behavior.

Magnetic phenomena in chemical substances may arise from both electrons and nuclei. However, the magnetic effects due to electrons are of the order of 10^3 times greater than those due to nuclei. Therefore, the magnetic phenomena associated with or arising from electrons alone will be of interest to chemists.

An electron may be considered, in effect, an elementary magnet. The origin of its magnetism is most easily described

in classical, that is, pre-wave mechanical terms, where we may picture the electron as a hard, negatively charged sphere that is both spinning on its axis and traveling in a closed path about a nucleus. The former motion gives rise to the spin moment and the latter to the orbital moment of the electron, and some combination of these two moments results in the paramagnetic moments found for certain atoms, ions, or molecules. These are expressed in Bohr Magneton (BM) units, where

$$\text{I.1} \qquad BM = eh/4\pi mc = 0.927 \times 10^{-20} \text{ erg/Oe.}$$

Here e is the electronic charge, h is Planck's constant, m is the electron rest mass, and c is the speed of light. The spin-only magnetic moment of a free electron μ_s, is given by wave mechanics as

$$\text{I.2} \qquad \mu_s \text{(in BM units)} = g\sqrt{s(s+1)}$$

where s is the absolute value of the spin quantum number and g is called the gyromagnetic ratio or Lande splitting factor. For the free electron g has the value 2.0023, which is generally taken simply as 2.00.

It is now necessary to consider how the orbital and spin momenta of the electrons of an atom are combined to form the atom's moment. The method of combination is known as Russell-Saunders coupling.

Just as l is used, as $[(l\,(l+1)]^{1/2}$, to indicate the angular momentum of a single electron, there is a quantum number L such that $[(L(L+1)]^{1/2}$ gives the total orbital angular momentum of the atom. Similarly, we use a quantum

number S to represent the total electron spin angular momentum given by $[S(S+1)]^{1/2}$, in analogy to the quantum number s for a single electron. There is the difference here in that while s is limited to the value 1/2, S may take any integral or half-integral value beginning with 0. Finally, just as the l and s value may couple (spin-orbital interaction) to give a j for a single electron, so the S and L values may couple to give a series of J values for all of the electrons. J is called the total angular momentum quantum number.

The value of g for an unpaired electron in a gaseous atom or ion where Russell-Saunders coupling is applicable, is given by the Lande formula*

$$\text{I.3} \qquad g = 1 + \frac{S(S+1) - L(L+1) + J(J+1)}{2J(J+1)}$$

where S, L, and J have their usual meaning. Note that for the free electron with no orbital angular momentum (that is, L = 0), J = S, and then g = 2.

I.2.1 Magnetic Susceptibility and Types of Magnetic Behavior.

Magnetic materials may be divided into six main groups, according to their magnetic properties, i.e.

(1) Diamagnetic
(2) Paramagnetic
(3) Ferromagnetic
(4) Ferrimagnetic
(5) Antiferromagnetic
(6) Metamagnetic

*The equation has been derived on pp. 164 and 370 of M. Born and K. Huang, Dynamical Theory of Crystal Lattices, Oxford, 1954.

Clearly such a division is an oversimplification and the most obvious example is the case of a ferromagnetic or ferrimagnetic material that becomes paramagnetic above a certain temperature. Behavior of these materials will be discussed later.

When a substance is placed in a magnetic field of strength H, the flux or magnetic induction, B, within the substance is given as

$$I.4 \qquad B = H + 4\pi I$$

where I is termed the intensity of magnetization. Dividing both sides of Eq. I.4 by H yields

$$I.5 \qquad B/H = 1 + 4\pi \frac{I}{H} = 1 + 4\pi k$$

where the ratio B/H is called the magnetic permeability of the substance and k is the magnetic susceptibility per unit volume.

Now when a substance is placed in an inhomogeneous magnetic field, it experiences a force F, which is proportional to the field strength, H, to the gradient of the field, $\partial H/\partial y$, and to the sample volume V. Mathematically we may express this as follows

$$I.6 \qquad F = kVH \frac{\partial H}{\partial y}$$

since we more often deal with the weight of solids rather than their volume, it is useful to define the specific or gram susceptibility, χ_g , and the molar susceptibility, χ_M , by the following relations

I.7 $$\chi_g = \frac{k}{\rho} \quad \text{and} \quad \chi_M = \frac{kM}{\rho}$$

where ρ is the density and M the formula weight of the compound.

I.2.2 Paramagnetism, Ferromagnetism, Ferrimagnetism, Antiferromagnetism, and Diamagnetism

(A) Paramagnetism

In his 1895 paper Curie showed that a certain class of substances had a temperature-dependent and field-independent susceptibility given by

I.8 $$\chi = \frac{C}{T}$$

where T is the absolute temperature and C is now called the Curie constant. The types of susceptibility observed by Curie is now known to occur only for substances that contain permanent magnetic dipoles. Later experiments showed that not all paramagnetic materials obey Curie's law. Some have susceptibilities that can be fitted to the equation

I.9 $$\chi = \frac{C}{T - \theta}$$

where θ is known as the Weiss constant. This equation is known as the Curie-Weiss law.

When χ_M is determined for a paramagnetic substance, it is necessary for precise work to correct the value for the diamagnetism of the constituent atoms. After the appropriate corrections for diamagnetism have been made, we then write the susceptibility χ_M^{corr} .

A quantum mechanical treatment of interaction between an applied magnetic field and the elementary permanent moments yields the expression for the total molar magnetic susceptibility

$$\text{I.10} \qquad \chi_M^{corr} = \frac{N\mu^2}{3KT}$$

where N is avogadro's number, K is Boltzman's constant and μ is the permanent magnetic moment in BM units. On rearranging Eq. I.10 and evaluating the constants, the magnetic moment can be expressed as

$$\text{I.11} \qquad \mu_{eff} = 2.84(\chi_M T)^{1/2} \quad \text{BM}$$

In an atom composed of many electrons the orbital angular moments of the variously oriented orbits combine vectorially to give the resultant orbital angular momentum of the atom, which is characterized by the quantum number L. Similarly, the individual electron spin momenta combine to give the resultant spin momentum, described by the quantum number S. Finally, the original and spin momenta of the atom combine to give the total angular momentum of the atom, described by the quantum number J. Then the net magnetic moment of the atom, usually called the effective moment μ_{eff}, is given in terms of g and J, as

$$\text{I.12} \qquad \mu_{eff} = g\sqrt{J(J+1)}\,\mu_B$$

The moment may be said to be made up of an effective number n_{eff} of Bohr Magnetons:

$$\text{I.13} \qquad n_{eff} = g\sqrt{J(J+1)}.$$

At this point the calculation of the net magnetic moment of an atom would seem straightforward, simply by a combination of Eqs. I.3 and I.12. However, the values of J, L, and S are known only for isolated atoms; it is, in general, impossible to calculate μ for the atoms of a solid, unless certain simplifying assumptions are made. One assumption, valid for many substances, is that there is no orbital contribution to the moment, that is, L = 0, therefore J = S. The orbital moment is, in such cases, said to be quenched.

When an atom forms part of, for example, a cubic crystal the orbits of this atom are in a sense bound, or coupled rather strongly to the crystal lattice. The spins, on the other hand, are only loosely coupled to the orbits. Thus, when a magnetic field is applied along some arbitrary direction, the strong orbit-lattice coupling often prevents the orbits, and their associated orbital magnetic moments, from turning toward the field direction, whereas the spins are free to turn because of relatively weak spin-orbit coupling. The result is that only the spins contribute to the magnetization process and the resultant magnetic moment of the specimen. Quenching may be complete or partial.

(B) Diamagnetism

Diamagnetism is a property of all forms of matter. It arises from the interaction of the applied magnetic field with the field induced in the complete shells of electrons.

When an atom or molecule is placed in a magnetic field, a small magnetic moment directly proportional to the strength of the field is induced. The electron spins have nothing to do with this induced moment; they remain tightly coupled together in antiparallel pairs. However, the planes of the orbitals are tipped slightly so that a small net orbital moment is set up in opposition to the applied field. It is because of this opposition that diamagnetic substances are repelled from magnetic fields. Hence, the diamagnetic susceptibility is a negative quantity, and from both a classical and a quantum mechanical treatment the diamagnetic susceptibility of any poly-electron atom is found to be a function of the average squared radius of its electrons:

$$\text{I.14} \qquad \chi_A = -\frac{Ne^2}{6mc^2} \sum_i \overline{r_i^2} = -2.83 \times 10^{10} \sum_i \overline{r_i^2}$$

where χ_A is the atomic susceptibility per cm^3, N is the number of atoms per cm^3, $\overline{r_i}^2$ is the average squared radius of the electron, m is electron rest mass, e is the electronic charge, and c is the velocity of light. From equation I.13, it is apparent that the diamagnetism will be very sensitive to change in the value of $\overline{r_i}^2$. Thus, both an increase in the size of an atom or ion as well as an increase in the number of electrons, i, will increase the magnitude of diamagnetic susceptibility. Temperature has no effect upon diamagnetism, nor does the magnitude of the applied field.

The magnitude of the diamagnetic effect is normally 10 to 1000 times less than that of the paramagnetic effect.

Therefore, its importance in most inorganic systems is primarily as a correction required for precise work. All substances that do not have the necessary electronic and structural features to give rise to para-, ferro-, antiferro-, or ferrimagnetism will necessarily exhibit only diamagnetism.

(C) Ferromagnetism

Ferromagnetism is a phenomenon which occurs especially in the metals iron, Gd, cobalt and nickel at room temperature. It occurs also in many alloys, including some whose separate constituent elements are not ferromagnetic: and it is also found in spinel $CdCr_2Se_4$, etc. The rare earth elements are also ferromagnetic at lower temperature. A spontaneous magnetization exists in such materials; that is, even in the absence of a magnetic field there is a magnetic moment. Above a critical temperature, T_c, called the Curie temperature, the spontaneous magnetization vanishes. The material is then paramagnetic with a susceptibility given by Curie-Weiss law (Eq. I.9) with a positive value of θ .

It is known that in spite of the spontaneous magnetization property a ferromagnetic specimen may exhibit no magnetic moment when the applied field is zero. However, the application of even a small field usually produces a magnetic moment which is many orders of magnitude larger than that produced in a paramagnetic substance. Weiss postulated that a ferromagnetic substance under no external field is divided into a number of small regions called domains. Each domain is spontaneously magnetized. But the direction of

magnetization of various domains are such that the specimen as a whole has no net magnetization. The application of an external field of the order of 1 to 100 oeresteds may often be sufficient to remove the domain structure and to bring the material practically to saturation; that is, the magnetization M of material reaches the constant value M_s.

Another typical property of ferromagnetics is the occurrence of hysteresis, that is, each value of the field H is not associated with one specific value of the induction B, but rather B depends upon the previous history of the specimen, that is upon the field which has been applied previously. For example, with a given field the induction will be larger if the material is first saturated in a strong field in the direction of H than if the material were first saturated in the opposite direction. The graph that shows the relation between B and H is known as the hysteresis loop (Fig. I.1).

As the applied field, H, is increased, B begins to increase slowly. Then the slope increases sharply and B rapidly rises until the saturation induction, B_s, is attained. With further increase in the field, the curve levels off. Upon decreasing the field, the original curve is not retraced. At zero H, the specimen is still magnetized and $B=B_r$, the remanent induction. At $B = 0$, $H = H_c$, the coercive force. If H is now made negative and the specimen saturated in the reverse direction before returning to zero field, the symmetric curve shown in Fig. I.1 is obtained with saturation, coercive force, and remanence equal to those on the positive

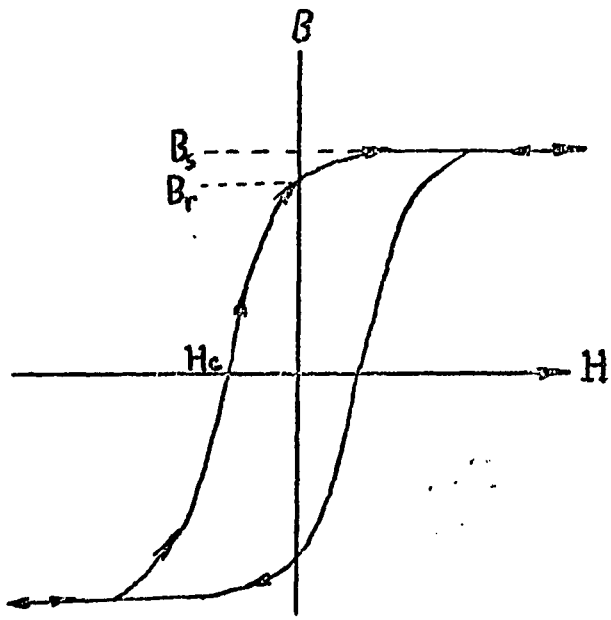

Fig. I.1 B vs H hysteresis loop for a ferromagnetic material.

side. Such irreversible, double-valued hysteresis behavior is characteristic of the magnetic behavior of ferromagnetic materials.

(D) Ferrimagnetism

A ferrimagnetic material may be defined as one which below a certain temperature possesses a sponteneous magnetization that arises from a nonparallel arrangement of magnetic moments of the constituent paramagnetic ions. The example originally considered was that of a substance composed of two sublattices with the magnetic moments of one sublattice tending to be antiparallel to those of the other. When the sublattice magnetizations are not equal there will be a net magnetic moment. The concept of ferrimagnetism has been broadened to include materials with more than two sublattices and with other spin configurations, such as garnet.

The most important ferrimagnetic substances are certain double oxides of iron and another metal, called ferrites, of which Fe_3O_4 is an example. Magnetite, Fe_3O_4 has the inverse spinel structure, $(Fe^{3+})[Fe^{2+}\ Fe^{3+}]O_4$ where the parentheses signify four-fold tetrahedral coordination, and the brackets six-fold octahedral coordination. Fe^{3+} ions are in the state with S = 5/2 and zero orbital moment, that is, L = 0, therefore J = S. Then each ion should contribute $5\mu_B$, because for each ion the number of BM is gJ and for Fe^{3+} g is 2. The ferrous (Fe^{2+}) ions have a spin of 2 and should contribute $4\mu_B$, apart from any residual orbital moment contribution.

Thus the effective number of Bohr Magnetons per Fe_3O_4 formula unit should be about 2X5 + 4 = 14 if all spins were parallel. The observed value is 4.1. The discrepancy is accounted for if the moments of Fe^{3+} ions on the two crystallographic sites are antiparallel to each other. Then the observed moment arises only from the Fe^{2+} ion.

(E) Antiferromagnetism and Metamagnetism

In an antiferromagnetic compound the spins are ordered in antiparallel arrangement. Néel originally considered an antiferromagnetic substance as composed of two sublattices, one of whose spins tends to be antiparallel to those of the other. He assumed the magnetic moment of the two sublattices to be equal, so that the net moment of the material was zero. Since Néel's original hypothesis the term antiferromagnetism has been extended to include materials with more than two sublattices.

Antiferromagnetic substances have a small positive susceptibility at all temperatures but their susceptibilities, χ, vary with temperature. As the temperature decreases, χ increases but finally goes through a maximum at a critical temperature, T_N, called the Néel temperature. The substance is paramagnetic above T_N and antiferromagnetic below it. T_N commonly lies far below room temperature, so that it is often necessary to carry susceptibility measurements down to quite low temperatures to discover if a given substance, paramagnetic at room temperature, is actually antiferromagnetic at some lower temperature.

For an antiferromagnetic substance a plot of $1/\chi$ versus T is a straight line above T_N and that this line extrapolates to a negative temperature at $1/\chi = 0$. In other words, the material obeys a Curie-Weiss law but with a negative value of θ.

Certain materials which are antiferromagnetic in weak applied fields behave in an unexpected fashion when the applied field is increased. The magnetization, which is small in weak fields, increases rapidly at a critical value of the applied field, and becomes saturated as all the magnetic moments in the material become aligned with the magnetic field. Such behavior is known as metamagnetism, and materials which behave in this way in applied magnetic field are called metamagnetic.

I.3 Garnet

I.3.1 The Garnet Structure. The garnet structure (space group Ia3d) was originally determined by Menzer (1, 2) for the naturally occurring garnets such as grossularite $Ca_3Al_2(SiO_4)_3$, uvarovite, $Ca_3Cr_2(SiO_4)_3$, and pyrope $Mg_{1.6}Fe_{1.2}Ca_{0.2}Al_2(SiO_3)_3$.

(A) Cation Sites

Garnets have the general chemical formula of $\{C_3\}[A_2](D_3)O_{12}$, with eight formula units per unit cell. Therefore, there are 96 sites (known crystallographically as h-sites) which are occupied by oxygens. The notation in the formula

designates the type of oxygen coordination polyhedra formed about each C, A and D cation. The cation sites in the garnet structure are classified into three types of sites (Table I.2). They are:

1. Tetrahedral sites: Each tetrahedral or d-site (indicated by ( )), is surrounded by 4 h-sites at the corners of a tetrahedron. There are 24 d-sites in each unit cell. Each d-site has the point symmetry group of $\bar{4}$ (S_4).

2. Octahedral sites: Each octahedral or a-site (indicated by [ ]), is surrounded by 6 h-sites at the corners of an octahedron. There are 16 a-sites in each unit cell of garnet. Each a-site has the point group of $\bar{3}$ (S_6).

3. Dodecahedral sites: Each dodecahedral or c-site (indicated by { }), is surrounded by 8 h-sites at the corners of a triangular dodecahedron (distorted cube). A triangular dodecahedron is a polyhedron which has 12 faces with each phase a triangle. There are 24 c-sites in each unit cell of garnet. Each c-site has the point group of 222 (D_2).

Each d-site is surrounded by 4 d-sites, 4 a-sites, and 6 c-sites. Each a-site is surrounded by 8 a-sites at the corners of a body-centered cube. It is also surrounded by 6 d-sites and 6 c-sites. Each c-site is translated one-fourth of the lattice constant distance from its contracting d-site.

(B) Polyhedra

As was discussed in the previous section on cation sites, the garnet structure has three types of cation sites, and, therefore, three types of polyhedra. The three types of

Table I.1: Description of garnet structure (Ref. 6).

Point Symmetry	222	3	4	1
Space Group Position	24c	16a	24d	96h
Typical Formula	Ca_3	Al_2	Si_3	O_{12}
Coordination to O	8	6	4	
Type of Polyhedron	Dodecahedron Distorted Cube	Octahedron	Tetrahedron	

polyhedra are triangular dodecahedra (distorted cube), octahedra, and tetrahedra, corresponding to the c-site, a-cite, and d-site respectively. Figs. I.2a-c show the three types of polyhedra in yttrium iron garnet $\{Y_3\}\ [Fe_2](Fe_3)O_{12}$.

The garnet structure as a network of tetrahedra and octahedra and eight-fold triangular dodecahedra is partially shown in Fig. I.3. Tetrahedra and octahedra are drawn with shaded lines, and the triangular dodecahedra are drawn as distorted cubes. In Fig. I.3, large open circles represent oxygens, the smaller circles are (D) cations and the hatched ones are $\{C\}$ cations.

The placement of a set of polyhedra onto the cubic lattice of rare earth iron garnet is shown in Fig. I.4. This figure fails to show that the tetrahedron shares two edges with dodecahedra and two edges with octahedra. Another fact that cannot be seen from the drawing is that no two tetrahedra have common corners.

(a)

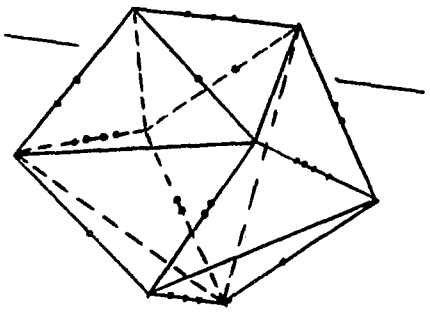

(b)

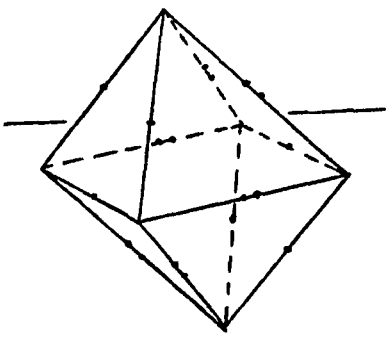

(c)

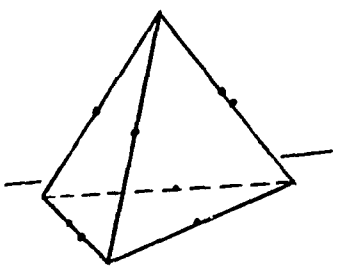

Figure I.2 Yttrium iron garnet
(a) Coordination polyhedron of oxygen ions about the yttrium ion (• 2.68, .. 2.81, ... 2.87, ... 2.97 Å).
(b) Coordination octahedron of oxygen ions about an Fe^{3+}(a) ion (. 2.68, .. 2.99 Å).
(c) Coordination tetrahedron of oxygen ions about an Fe^{3+}
(d) ion (. 3.16, .. 2.87 Å).

(Geller and Gilleo, Ref. 4)

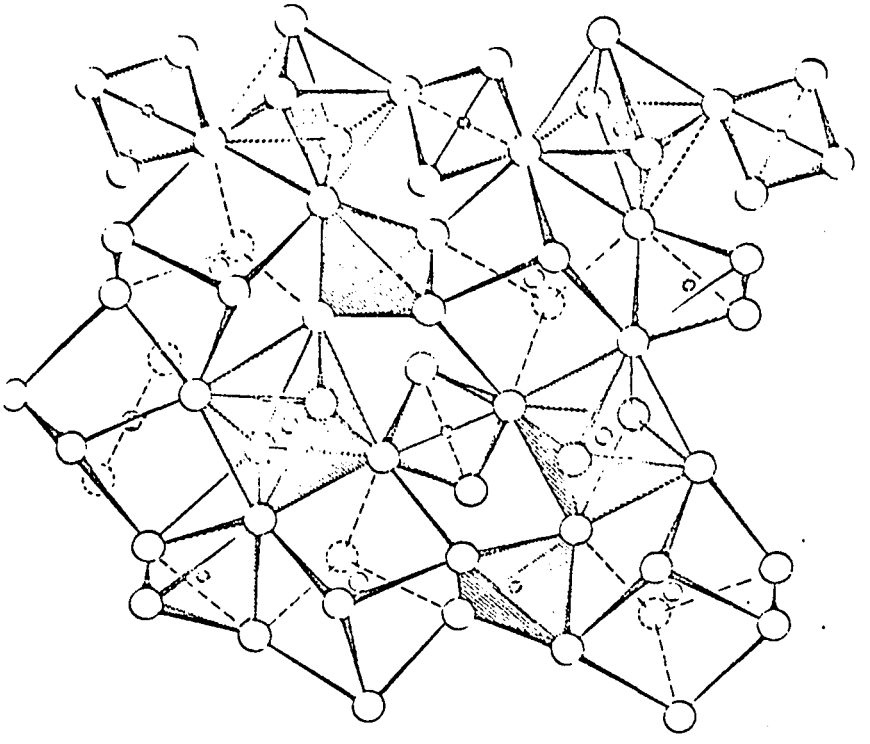

Fig. I.3. Garnet structure as a network of tetrahedra octahedra, and eightfold triangular dodecahedron . (ref. 5)

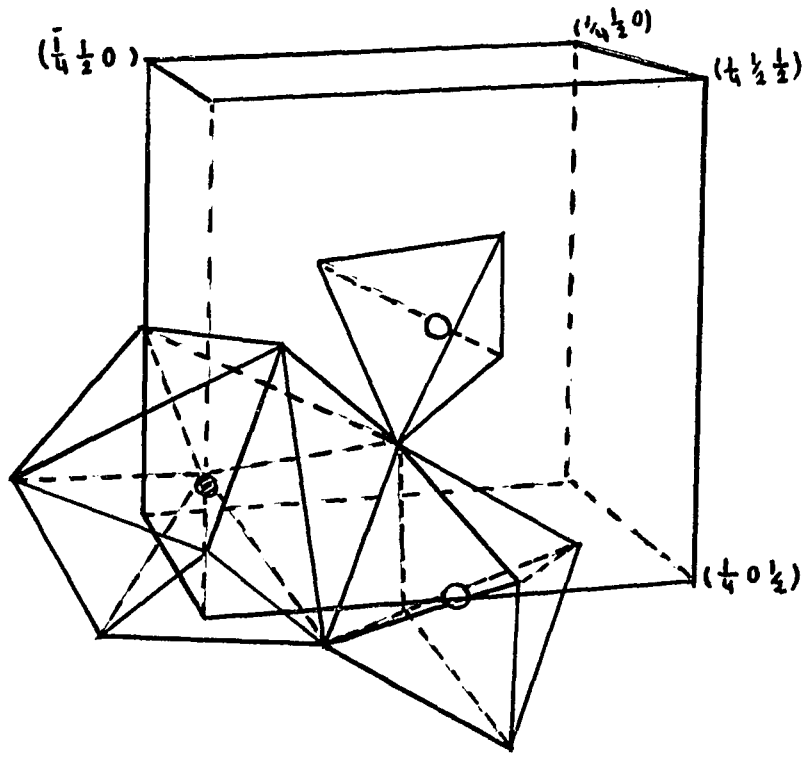

Fig. I.4. A portion of the garnet structure consisting of one tetrahedron, one octahedron, and one triangular dodecahedron. (ref. 6)

Fig. I.5, shows a portion of the garnet structure consisting of one tetrahedron, one octahedron, and two triangular dodecahedra. The {C} cations are marked X(1) and X(2), the [A] cation Y, and the (D) cation Z in Fig. I.5.

The surroundings of a {C} cation in a triangular dodecahedron are shown in Fig. I.6 with its six neighboring (D) cations. The open circle represents the {C} cation, the vertices of the dodecahedron are the oxygen positions, and the solid circles are the (D) cations.

I.3.2 Synthetic Garnets. A new era for scientific and technological exploration of the garnets was opened by discovery of ferrimagnetic yttrium iron garnet $\{Y_3\}[Fe_2](Fe_3)O_{12}$, abbreviated YIG.

The history of magnetic iron garnets began with an error in the interpretation of experimental results. In 1950 the perovskite structure with composition $Me^{3+}Fe^{3+}O_3$ was incorrectly allocated to the magnetic "rare-earth ferrites" (8). Bertaut and Forrat (9) in 1956 and Geller and Gilleo in 1957 (10) showed independently that the real magnetic phase was the garnet structure $Me^{3+}Fe_5^{3+}O_{12}$, which coexisted with a nonmagnetic phase $Me^{3+}Fe^{3+}O_3$ with perovskite structure. In fact the orthoferrites of rare earths $Me^{3+}Fe^{3+}O_3$ are antiferromagnetic.

A very large number of substituted garnets have been produced and investigated, because if cations of proper size are chosen so that the total charge of cations in c, a, and d sites is 24+ and the ratio of ions are 3:2:3:12 one

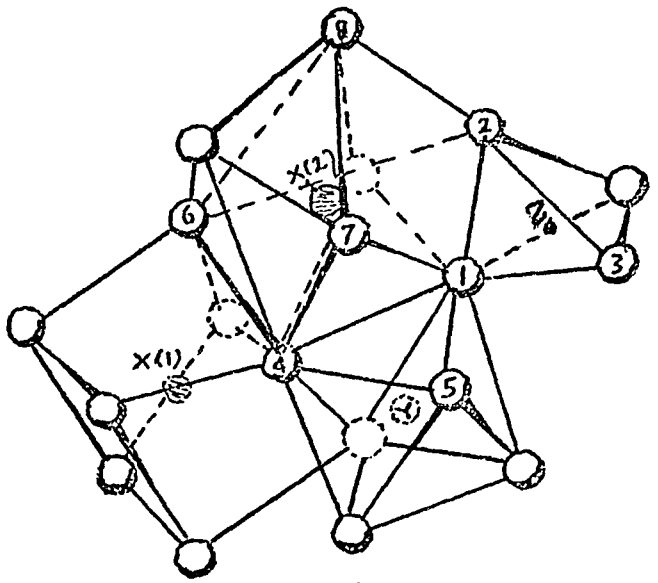

Fig. I.5. A portion of the garnet structure consisting of one tetrahedron, one octahedron, and two triangular dodecahedra. (ref. 7)

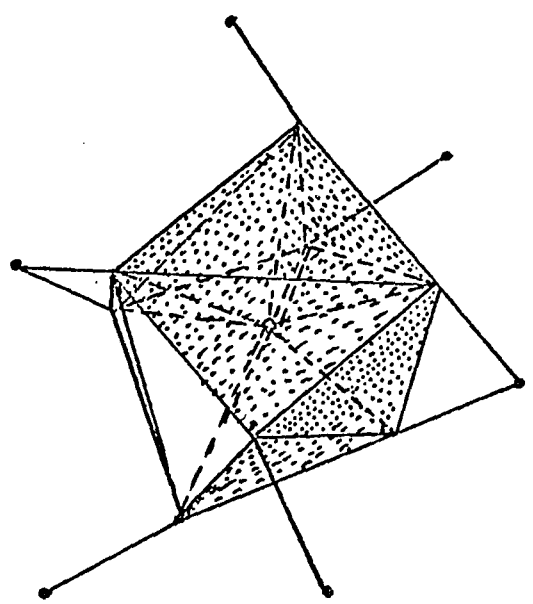

Fig. I.6. Surroundings of a dodecahedral site, or c-site in garnet. (ref. 7)

possibly can prepare a new substance with garnet structure. Five importantgroups of garnet compounds are

Silicate Garnets

Germanium Garnets

Aluminum Garnets

Gallium Garnets

Iron Garnets.

These five groups are all oxygarnets. Fluoride ions have been used either to replace oxygen completely, as in the case of $\{Na_3\}\ [Al_2](Li_3)F_{12}$, (11) or partially, as in the case of $\{Y_3\}\ Fe_{5-x}M_xO_{12-x}F_x$ (M=3d transition elements) (12).

I.3.3 Silicate Garnets. The silicate garnets are listed in Table I.2. Many of these garnets have been made by hydrothermal techniques. Spessartine ($Mn_3Al_2Si_3O_{12}$) is synthesized by melting a mixture of the appropriate amounts of reactant oxides at a temperature of 1200-1250°C. When cooled, a glass is obtained which is then annealed at 1800°C for 18 hours. Synthetic uvarovite ($Ca_2Cr_3Si_3O_{12}$) may be obtained by solid state reaction.

Table I.2 End-member silicate garnets $\{A_3\}\ [B_2](Si_3)O_{12}$ (Ref.3)

A^{2+}	B^{3+}	a (Å)	References
Mg	Al	11.459	13, 14, 15
	Cr	not reported	14

Table 1.2 (Continued)

A^{2+}	B^{3+}	a(Å)	References
	Fe	not reported	14
Ca	Al	11.851	15
	Sc	12.27	16
	V	12.09, 12.07 12.068	16, 17, 18
	Cr	12.00, 11.999	19, 20
	Fe	12.059, 12.067	21, 22
	Ga	12.00	23
	In	12.35	16
Mn	Al	11.621	15, 24
	Fe	11.82	14, 25
Fe	Al	11.526	15
Co	Al	11.471	26
Cd	Al	11.820	27
	V	12.09	16

I.3.4 Germanate Garnets. The germanate garnets are listed in Table I.3. Mill (16) has synthesized some germanates hydrothermally but all the germanate garnets can be made by solid-state reaction including $Mn_3V_2Ge_3O_{12}$.

Table I.3 Lattice constant of several germanate garnets (Ref. 3, 28)

Composition	a(Å)	Composition	a(Å)
$Ca_3Zr_2Ge_2Co'O_{12}$	12.62	$Ca_3Al_2Ge_3O_{12}$	12.12
$Ca_3Sn_2Ge_2Co\ O_{12}$	12.52	$Ca_3Sc_2Ge_3O_{12}$	12.504
$Ca_3Zr_1Mg\ Ge_3O_{12}$	12.50	$Ca_3V_2Ge_3O_{12}$	12.350
$Ca_3SnMg\ Ge_3O_{12}$	12.44	$Ca_3Cr_2Ge_3O_{12}$	12.265
$Ca_3TiMg\ Ge_3O_{12}$	12.35	$Ca_3Dy_2Ge_3O_{12}$	12.83
$Ca_3ZrCo\ Ge_3O_{12}$	12.52	$Ca_3Ho_2Ge_3O_{12}$	12.81
$Ca_3SnCo\ Ge_3O_{12}$	12.46	$Ca_3Er_2Ge_3O_{12}$	12.785
$Ca_3TiCo\ Ge_3O_{12}$	12.35	$Ca_3Tm_2Ge_3O_{12}$	12.765
$Ca_3ZrNi\ Ge_3O_{12}$	12.49	$Ca_3Yb_2Ge_3O_{12}$	12.74
$Ca_3SnNi\ Ge_3O_{12}$	12.43	$Ca_3Lu_2Ge_3O_{12}$	12.73
$Ca_3TiNi\ Ge_3O_{12}$	12.335	$Sr_3Sc_2Ge_3O_{12}$	12.785
$Y_2Mg_3Ge_3O_{12}$	12.21	$Sr_3In_2Ge_3O_{12}$	12.87
$Y_2MgCo_2Ge_3O_{12}$	12.23	$Sr_3Y_2Ge_3O_{12}$	13.085
$Y_2Co_3Ge_3O_{12}$	12.26	$Sr_3Ho_2Ge_3O_{12}$	13.09
$Y_2CaMg_2Ge_3O_{12}$	12.31	$Sr_3Er_2Ge_3O_{12}$	13.065
$Y_2CaCo_2Ge_3O_{12}$	12.35	$Sr_3Tm_2Ge_3O_{12}$	13.04
$Gd_3Mn_2Ge_2Ga\ O_{12}$	12.550	$Sr_3Yb_2Ge_3O_{12}$	13.03
$Mn_3Al_2Ge_3O_{12}$	11.902	$Sr_3Lu_2Ge_3O_{12}$	13.01

I.3.5 Rare earth aluminum, iron, and gallium garnets.

Lattice constants for these garnets are listed in Table I.6. The broad attention to these groups originated from the discovery of ferrimagnetism in the case of iron garnets.

Table I.4 Rare earth aluminum, iron and gallium garnets (Ref. 3)

$\{A_3\}[B_2](C_3)O_{12}$

A	B, C	a(Å)*
Y	Al	12.01, 12.02, 12.000, 12.000
Gd		12.11, 12.113, 12.111
Tb		12.074
Dy		12.06, 12.042
Ho		12.011
Er		11.98, 11.981
Tm		11.957
Yb		11.929
Lu		11.912
Y	Fe	12.376
La**		12.767
Nd**		12.60, 12.596, 12.600
Pm**		12.57
Sm		12.524, 12.530, 12.528, 12.529
Eu		12.518, 12.498
Gd		12.479, 12.472, 12.471
Tb		12.447, 12.436
Dy		12.414, 12.405
Ho		12.380, 12.375
Er		12.349, 12.347
Tm		12.325, 12.323
Yb		12.291, 12.302
Lu		12.277, 12.283
Y	Ga	12.30, 12.273, 12.280, 12.275
Pr		12.57, 12.545
Nd		12.50, 12.506
Sm		12.355, 12.42, 12.433
Eu		12.402
Gd		12.39, 12.376
Tb		Not reported
Dy		12.32, 12.307
Ho		12.282
Er		12.25, 12.255
Tm		Not reported
Yb		12.204, 12.200
Lu		12.188, 12.183

* Different authors have reported different lattice constants for the same composition.

** Hypothetical.

I.3.6 Ferrimagnetic Garnets. Yoder and Keith (29) showed in 1951 that substitution can be made in the ideal mineral garnet $Mn_3Al_2Si_3O_{12}$. By substituting $Y^{III} + Al^{III}$ for $Mn^{II} + Si^{IV}$ they obtained the first silicon-free garnet, $Y_3Al_5O_{12}$. In 1956 Bertaut and Forrat (30) reported the preparation and magnetic properties of YIG and Geller and Gilleo, in 1957, (10) prepared and investigated $Gd_3Fe_5O_{12}$, which compound is also ferrimagnetic. It appeared (30) that the Y-ion could be replaced by the rare earth ions Sm, Eu, Gd, Tb, Dy, Ho, Er, Tm, Yb, or Lu (Table I.4) but it is not possible to replace all the yttrium by larger rare earths such as Nd, Pr, and La.

The ferric ions on the octahedral (a) and tetrahedral (d) sites are coupled antiferromagnetically by super exchange mechanism as in the other ferrites. Since there are two octahedral and three tetrahedral ferric ions per formula unit, $\{M_3\}[Fe_2](Fe_3)O_{12}$, there will be a net magnetic moment equivalent to one ferric ion ($5\mu_B$) per formula unit from these two sublattices. If the rare earth ion in the c-site is nonmagnetic (e.g., Lu^{3+}), there is no further magnetic contribution to the net moment of the a-d interaction. For other rare earths the magnetization of the rare earth sublattice is aligned antiparallel to the net ferric moment of a and d sites (Fig. I.7).

There is the possibility that the c-sublattice magnetization and net ferric magnetization might exactly cancel. In fact, $\{Yb_3\}[Fe_2](Fe_3)O_{12}$ shows just such a cancellation near absolute zero. The magnetization is then said to be compensated. Such compensation points ($T_{comp.}$) are characteristic of many garnets.

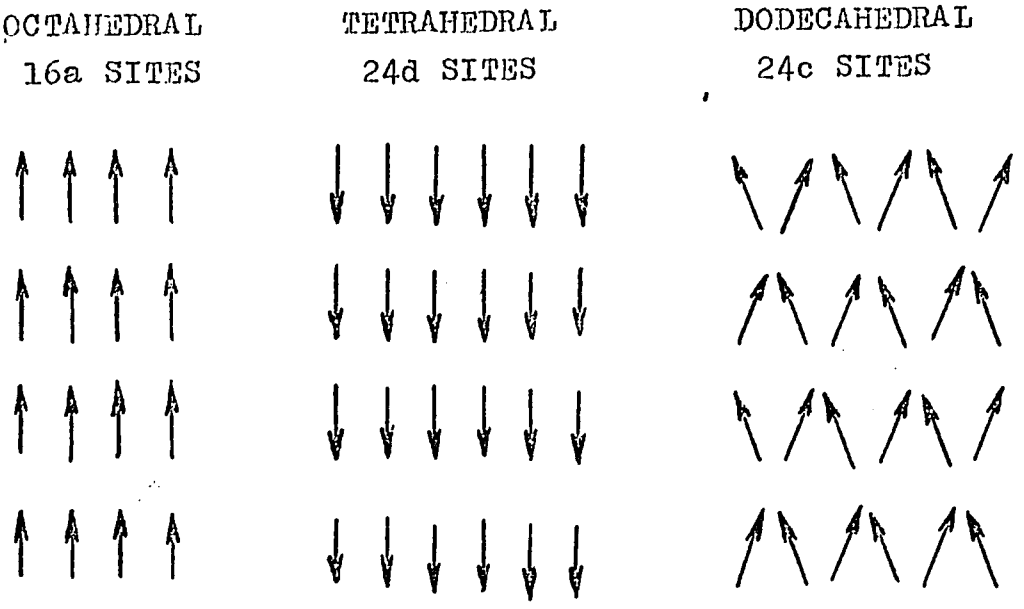

Fig. I.7 Disposition of magnetic moments in rare earth garnets (for light rare earth ions, Pr through Sm, the moments on the 24c sites point downwards)

The magnetization of rare earth ions drops very quickly with increasing temperature, approximately as 1/T. Eventually, the temperature becomes high enough for the a-d interaction to be overcome as well, and the material becomes paramagnetic. The presence or absence of a magnetic rare earth ion has little effect on the Curie point (T_c).

Most of the rare earth ions have relatively large magnetic moments, and dominate the magnetization at low temperature. As the temperature is raised and c-sublattice magnetization diminishes, a compensation point is reached, beyond which the ferric moment dominates.

I.3.7 Other than octahedral-tetrahedral ion interaction in the garnet structure. Geller and others unsuccessfully tried to prepare garnet $\{Mn_3\}[Fe_2](Si_3)O_{12}$ in which dodecahedral and octahedral sites would be filled by magnetic ions. Coes (31) succeeded in preparing this at high pressure by the hydrothermal method. The magnetic measurements of these compounds were disappointing at 0°K; the spontaneous magnetization was only 0.1 μ_B. A number of germanium garnets including $\{Mn_3\}[Fe_2](Ge_3)O_{12}$ were discovered by Tauber et al (32). This garnet was found to be only antiferromagnetic at low temperature.

Geller and Gilleo (33) found garnets $\{M^{2+}Gd_2\}[Mn_2](Ge_3)O_{12}$ (where M=Mn and Ca) to be ferrimagnetic at 6°K or lower. They carried out more definite measurements on $\{Gd_3\}[Mn_2](GaGe_2)O_{12}$, which was found to have a Curie temperature of

8°K and a saturation magnetization of 9.6 μ_B at 0°K. The fact that the Gd-O-Mn interaction is stronger than Mn-O-Fe interaction is especially interesting because one might tend to consider rare earth ions to be less capable of ferrimagnetic interactions because the participating electrons of Gd^{3+} are in inner f-shells.

The magnetic moment of $\{Gd_3\}[Mn_2](Ge_2Ga)O_{12}$ was measured by Geller and Gilleo (34) as a function of H at constant T. These curves showed no saturation at high field because T_c (the Curie temperature) is sufficiently low so that the applied field is of the order of magnitude of the Weiss molecular (or exchange) field, The spontaneous magnetization for H=0 therefore was obtained by extrapolation under the assumption that $n_B(H, T) = n_B(0, T) + \chi(T)H$ is a reasonable approximation to the nearly linear portion of the curves. On this basis $n_B(0, 0)$ is about 9.6 μ_B.

I.3.8 Rare earth garnets with trivalent rare earth ions on both dodecahedral and octahedral sites. On studying double oxides of trivalent elements, Keith and Roy (35) found that many ABO_3 compositions assumed the perovskite structure if A is a large ion and B a small one. In several systems, however, the garnet structure was also observed, though usually accompanied by perovskite or distorted perovskite phases when the starting composition of oxides was equimolar. These systems were Y_2O_3 - Al_2O_3, Ce_2O_3 - Ga_2O_3, Nd_2O_3 - Ga_2O_3, and Sm_2O_3 - Ga_2O_3. The garnet structure was obtained with 1:1 compositions apparently because solid solutions like $\{Y_3\}[Y, Al_2](Al_3)O_{12}$

form. Results rather similar to these but differing somewhat in detail, were obtained by Roth (36) in the Y_2O_3 - Al_2O_3 system. Schneider, Roth and Waring (37) investigated the extent of garnet solid solution formation in systems containing Ga_2O_3 with Nd_2O_3, Sm_2O_3, Eu_2O_3, Gd_2O_3, Dy_2O_3, Ho_2O_3, Er_2O_3, Tm_2O_3, Yb_2O_3, Lu_2O_3, or Y_2O_3 and also in systems containing Al_2O_3 along with either Yb_2O_3 or Lu_2O_3. In the gallium garnets, maximum solubility of rare earth on the octahedral sites was found at Tm^{3+} and fell off in both directions along the rare earth series. The formula of the composition with maximum Tm is $\{Tm_3\}[Tm_{0.8}Ga_{1.2}](Ga_3)O_{12}$.

Mill (38) prepared a large number of germanium garnets with large divalent alkaline earth ions (Ca and Sr) on the dodecahedral sites and small trivalent rare earth ions (Dy, Ho, Er, Tm, Yb, Lu, and also Sc and Y) on the octahedral sites (e.g., $\{Sr_3\}[Tm_2](Ge_3)O_{12}$ and $\{Ca_3\}[Yb_2](Ge_3)O_{12}$) by reaction of oxides at 1250°C.

Suchow, Kokta, and Flynn (39) studied the preparation of garnets of the type $\{Nd_{3-y}R_y\}[R_xGa_{2-x}](Ga_3)O_{12}$ in which R is Lu, Yb, Tm, Er, Ho, or Dy. It was found that the placement of large rare earth ion such as Nd^{3+} on the dodecahedral sites opens up the lattice so that small rare earth ions may enter the octahedral sites.

For the case of R=Lu (Table I.5) single-phase $\{Nd_3\}[Lu_2](Ga_3)O_{12}$ (i.e. y=0, x=2) was prepared. To prepare single-phase Yb and Tm compounds with x=2 it was necessary simultaneously to place determined minimum amounts of R in dodecahedral positions. This minimum required value of y increases with increasing radius of R.

Table I.5 Lattice constant of some neodymium garnets (Ref. 39)

$\{Nd_{3-y}R_y\}[R_{2-x}Ga_x](Ga_3)O_{12}$

R	y	x	Lattice Constant a(Å)
-	0.0	0.0	12.50_4
Yb	3.0	0.0	12.20_3
Lu	0.0	2.0	12.88_1
Yb	0.0	2.0	12.89_0
Tm	0.0	2.0	12.88_2
Er	0.0	2.0	12.83_1
Ho	0.0	2.0	12.65_2
Dy	0.0	2.0	12.51_0
Lu	0.2	2.0	12.86_6
Yb	0.3	2.0	12.86_4
Yb	0.5	2.0	12.85_5
Tm	0.6	2.0	12.85_4
Er	1.1	2.0	12.81_3

In another paper (40) Suchow and Kokta studied the preparation of garnets of the type $\{Pr_{3-y}R_y\}[R_xGa_{2-x}](Ga_3)O_{12}$. Table I.6 contains a list of lattice constants of these compounds.

Table I.6

$\{Pr_{3-y}R_y\}\ [R_xGa_{2-x}](Ga_3)O_{12}$*

R	y	x	Lattice Constant a(Å)
Lu	0.0	2.0	12.94
Yb**	0.0	2.0	12.92
Yb	0.5	0.0	12.50
Yb	0.5	2.0	12.89
Tm***	0.0	2.0	12.90
Tm	0.8	0.0	12.48
Tm	0.8	1.0	12.67
Tm	0.8	2.0	12.88
Er***	0.0	2.0	12.88
Er	1.15	0.0	12.43
Er	1.15	1.75	12.82
Er**	1.15	2.0	12.86

* Single phase unless otherwise noted.
** Almost single phase.
*** Nominal composition, not single phase.

The compounds which appear in Tables I.5 and I.6 were subjected to magnetic measurements (40, 41) over the temperature range 78-300°K and some also at 4.2°K and/or over the range 1.6-300°K. The materials were found to be paramagnetic with Curie-Weiss behavior, but in some the slopes of the $1/\chi$ vs T plots change at very low temperature.

II. EXPERIMENTAL STUDIES

II.1 Objectives

As stated above, the present work was oriented toward three subjects:

1. The confirmation by structure factor calculations of filling by rare earths of two crystallographic sites of the garnet structure.
2. Preparation of new rare earth garnets and study of their magnetic properties.
3. Attempts to prepare new rare earth apatites.

II.2 Preparations

All preparations were made by dissolving weighed stoichiometric quantities of desired oxides* in nitric acid and then gently boiling down to dryness. The residue is collected and heated for three hours at 500°C. in an open porcelain crucible in order to decompose the nitrates. This product is ground in an agate mortar and again heated, but now for 16 hours at 1350°C in an open platinum crucible. The resulting material is then ground once more in an agate mortar and heated 24 hours longer at 1350°C. The heating is in all cases carried out in air in a muffle furnace.

In some cases coprecipitation was employed as a step in the preparation. The oxides were first dissolved in

*Rare earth oxides were heated at 1000°K before they were used because it was found that some of them (expecially Nd oxide) pick up water on standing.

nitric acid and hydroxides were then precipitated using ammonium hydroxide. After filtration the hydroxides were air dried and heated at 500°C for three hours. This product was ground in an agate mortar and again heated, but now for 16 hours at 1350°C in an open platinum crucible. The resulting material was then ground once more in an agate mortar and heated 24 hours longer at 1350°C.

Where Ga was involved the quantitative coprecipitation of all hydroxides was impossible. All of the rare earths precipitate at pH=9 but gallium precipitates at a pH of about 6 and the gallium hydroxide starts to redissolve at a pH of about 7.

II.3 X-ray Diffraction Powder Patterns

The x-ray diffraction powder method using Norelco equipment with 57.3 mm radius powder cameras was the basic technique (except for two samples for confirmation of the filling by rare earths of two crystallographic sites of the garnet structure)* used to characterize the prepared compound. X-ray patterns obtained were checked to see whether they contained only lines belonging to the garnet structure.

The lattice constants were calculated according to the relationship for the cubic crystal structure

$$a = d\sqrt{h^2 + k^2 + 1^2}$$

*Quantitative intensity data was obtained with a General Electric Company XRD-6 unit with an SPG2 spectrogoniometer (diffractometer).

where d is the spacing between planes in the unit cell, and h, k and l are the Miller indexes of the planes. Four lines in the back reflection region of the powder pattern (i.e. (12 8 2), (12 6 6), (12 10 0), and (12 10 1) were used for lattice constant calculations. Lattice constant calculations were carried out by the Straumanis method.

III. CONFIRMATION BY STRUCTURE FACTOR CALCULATIONS OF THE FILLING OF TWO CRYSTALLOGRAPHIC SITES OF THE GARNET STRUCTURE (42)

III.1 Introduction

The filling of the octahedral sites of the garnet structure by rare earth when the same rare earth or larger rare earth ions also completely fill the dodecahedral sites was discussed in section I.3.6.

The general formula for the known compounds of this type may be taken as $\{M_{3-y}R_y\}[R_xA_{2-x}](A_2)O_{12}$, where M is the large rare earth, R the small one, and A either Ga or Al. The braces signify eight-fold dodecahedral coordination (a distorted cube), the brackets six-fold octahedral coordination, and the parentheses four-fold tetrahedral coordination.

In all the papers discussed (37-41), the presence of rare earth ions on octahedral sites was deduced from an observed increase in lattice constant and the fact that these ions had no other possible sites to enter in the garnet structure after the dodecahedral sites were filled. This argument is especially valid when the products are single-phase materials. Until now, however, there has been no direct confirmation of this picture by means of structure factor calculations; such confirmation was the purpose of this part of the dissertation. Two materials were chosen for the calculations: $\{Nd_{2.7}Yb_{0.3}\}[Yb_2](Ga_3)O_{12}$ and $\{Pr_3\}[Lu_2](Ga_3)O_{12}$.

III.2 X-ray Diffraction Powder Patterns

Although these two garnets with rare earth ions filling two crystallographic sites have x-ray patterns (obtained with Norelco equipment) quite similar to those of the rare earth garnets containing gallium on both octahedral and tetrahedral sites, there are a number of marked intensity shifts which should be accounted for by structure factor calculations if the assumed structures are correct. Most notable among such shifts in relative intensity are those in lines at $h^2 + k^2 + l^2 = 20$ and 24; 52 and 56; 80, 84 and 88; and 116 and 120. The 24-line does, in fact, become the strongest in the patterns of the materials with rare earths on two sites.

Quantitative intensity data for comparison with calculated intensities were obtained with a General Electric Company XRD-6 unit with an SPG2 spectrogonimeter (diffractometer). Values given in the tables are integrated intensities, taken by measuring areas under peaks.

III.3 Calculation of Structure Factors

The relative intensity of powder pattern lines can be calculated by the equation:

$$\text{III.1} \qquad I = |F|^2 \, P \, \frac{1 + \cos^2 2\theta}{\sin^2\theta \cos\theta}$$

where I = relative integrated intensity, F = structure factor, P = multiplicity factor (the number of different planes in a form having the same spacing (e.g., (100), (010), (001), ($\bar{1}$00),

(0T0), (00T)), and θ = Bragg angle $(1 + \cos^2 2\theta)/2$ Polarization factor, and $1/2 \sin^2\theta \cos\theta$ = Lorentz factor.

The garnet space group is Ia3d, for which the structure factor formula (43)

$$\text{III.2} \qquad F = \sum f_m S_m \qquad S_m = A + iB \qquad B = 0$$

$$A = 16\cos 2\pi(h + k + 1)/4 \cos 2\pi(hx + 1/4) \cos 2\pi(ky + h/4) \cos 2\pi(lz + k/4) + \cos 2\pi(kx + h/4) \cos 2\pi(ly + k/4) \cos 2\pi(hz + 1/4) + \cos 2\pi(lx + k/4) \cos 2\pi(hy + 1/4) \cos 2\pi(kz + h/4) + 1 \cos 2\pi(h + k + 1)/4 [\cos 2\pi(kx + 1/4) \cos 2\pi(hy + k/4) \cos 2\pi(lz + h/4) + \cos 2\pi(lx + h/4) \cos 2\pi(ky + 1/4) \cos\pi(hz + k/4) + \cos 2\pi(hx + k/4) \cos 2\pi(ly + h/4) \cos 2\pi(kz + 1/4)] .$$

In Eq. III.2 f_m is the atomic scattering factor (43) that can be calculated from

$$\text{III.3} \qquad f_m = f_0 e^{-M}$$

$$M = B \sin^2\theta / \lambda^2$$

B = Debye parameter

Table III.1 Multiplicities for powder method

h k l	Multiplicity Factor
h 0 0	6
0 k 0	6
0 0 1	6
h h 0	12
h 0 h	12
0 h h	12
h h h	8
h k 0	24
h 0 1	24
0 k 1	24

Table III.1 (Continued)

h k l	Multiplicity Factor
h h 1	24
h 1 h	24
1 h h	24
h k 1	48

To obtain calculated intensities (with an RCA System 3 Computer), the various ions were first assigned to tetrahedral, octahedral, and dodecahedral sites with various postulated distributions, and scattering factors (f) were taken from Ref. 44 for the trivalent cations and from Ref. 43 for the oxide ion. Appropriate corrections were made for multiplicity factors, Lorentz and polarization factors, and temperature factors (assuming for the Debye parameter, B, an overall isotropic value of 1.5, which is a rather average value for inorganic compounds). In Eq. III.1 the absorption factors were not included because they do not vary with θ when the data is obtained with an "infinitely thick" sample in a powder diffractometer. The x, y and z values for the oxide ions in general position 96(h) were taken as -0.025, +0.049, and +0.149, respectively; these are average values for garnets and were found, when used in a test, to give good calculated intensities for $Yb_3Ga_5O_{12}$, a compound whose x-ray pattern and observed intensities are known (45) and whose x, y and z values have been determined precisely as

-0.0259, +0.0563, and +0.1519, respectively (46). Variations of ± 0.01, ± 0.015, and ± 0.03 in the average values of x, y and z, respectively, were found not to cause any changes in calculated intensities of $Yb_3Ga_5O_{12}$ which were significant enough to have a serious effect on the comparison with powder data.

Results of full calculations are given in Tables III.2 and III.3. Included therein are calculations for the cation distributions indicated by the formula in section III.1 above as well as other distributions which do not really seem very logical from the viewpoint of crystal chemistry. These calculations confirm the earlier deduced structrual formula $\{Nd_{2.7}Yb_{0.3}\}[Yb_2](Ga_3)O_{12}$ and $\{Pr_3\}[Lu_2](Ga_3)O_{12}$. Because of a remaining possibility that there was partial, even if small, switching of large and small rare earths on the dodecahedral and octahedral sites, additional calculations were carried out for a number of such formulas but using only the nine key planes discussed in the x-ray diffraction powder patterns section above. The results given in Tables III.4 and III.5 indicate that there is no such switching. The R′ factors given in these tables are R factors calculated only from these nine lines. In cases where structural formulas are the same in Tables III.2 and III.4 or Tables III.3 and III.5, R and R′ are therefore slightly different. It is obvious, however, that agreement becomes poorer and progressively so as switching is postulated. The relative intensities of lines at $h^2+k^2+l^2=20$ and 24 are especially

sensitive to rare earth distribution and one can see very nicely, and perhaps even better than from the R factors, exactly the same trend simply by comparing the observed intensity of these two lines with the several calculated values. The calculations account very well for the observed intensity shifts in the x-ray patterns of the compounds with the previously deduced structures with rare earths on two crystallographic sites as compared with $\{RE_3\}[Ga_2](Ga_3)O_{12}$. Further improvement in both the R factors and the calculated intensities of the 8-lines can almost surely be brought about by refinement of the x, y and z values and also by determining good B values for the various ions on appropriate sites and then applying the resulting better temperature factors to the terms for the ions to which they pertain, rather than using overall values. Of course, best results would be obtained by comparison of calculated intensities with single crystal data.

Table III.2

Observed and Calculated Intensities of Allowable Lines in Nd-Yb Gallium Garnet ($a = 12.86_4$ Å)

		I_{calc} for Postulated Structural Formulae		
$h^2+k^2+\ell^2$	I_{obs}	$\{Nd_{2.7}Yb_{0.3}\}[Yb_2](Ga_3)O_{12}$	$\{Nd_{0.7}Yb_{2.3}\}[Nd_2](Ga_3)O_{12}$	$\{Nd_{2.7}Yb_{0.3}\}[Ga_2](Yb_2Ga)O_{12}$
6	9.8	13.3	18.0	0.1
8	7.2	17.2	4.3	7.7
14	6.1	7.2	10.4	0.0
16	52.9	60.6	48.7	22.1
20	97.7	94.0	100	100
22	-	0.1	0.5	0.7
24	100	100	78.5	32.8
26	1.3	1.1	1.0	0.7
30	7.5	7.5	9.2	0.8
32	-	0.9	0.0	2.8
38	7.8	7.5	9.1	0.8
40	5.2	5.1	1.6	1.1
42	-	0.0	0.0	0.0
46	2.4	1.1	1.6	0.0
48	5.9	5.1	7.9	15.0
50	-	0.0	0.0	0.0
52	27.0	25.2	26.4	25.7
54	3.0	3.0	4.0	0.0
56	68.6	64.6	51.7	23.0
62	1.3	1.6	2.3	0.1
64	18.6	18.4	16.7	11.2
66	-	0.1	0.0	0.1
68	-	0.1	0.1	0.1
70	-	0.4	0.7	0.0
72	1.6	1.8	0.4	1.0
74	-	0.0	0.0	0.0
78	-	0.4	0.6	0.0
80	15.9	15.5	12.3	5.4
84	16.6	15.0	16.1	16.4
86	1.2	1.2	1.6	0.0
88	12.2	12.3	10.1	4.4

Table III.2 (Continued)

Observed and Calculated Intensities of Allowable Lines in Nd-Yb Gallium Garnet (a = 12.86$_4$Å)

$h^2+k^2+\ell^2$	I_{obs}	I_{calc} for Postulated Structural Formulae		
		$\{Nd_{2.7}Yb_{0.3}\}[Yb_2](Ga_3)O_{12}$	$\{Nd_{0.7}Yb_{2.3}\}[Nd_2](Ga_3)O_{12}$	$\{Nd_{2.7}Yb_{0.3}\}[Ga_2](Yb_2Ga)O_{12}$
90	-	0.2	0.1	0.0
94	1.2	0.9	1.2	0.0
96	0.9	0.8	0.2	0.3
98	-	0.2	0.2	0.2
100	-	0.0	0.0	0.0
102	-	0.3	0.4	0.0
104	-	1.1	0.1	1.5
106	-	0.0	0.0	0.0
110	1.2	1.2	1.6	0.0
114	-	0.0	0.0	0.0
116	13.3	12.3	13.2	13.4
118	-	0.6	0.7	0.0
120	13.6	13.3	10.5	4.6
122	-	0.0	0.0	0.0
126	0.9	1.0	1.3	0.0
128	8.1	8.8	8.0	5.4
134	-	0.7	0.9	0.0
136	-	0.4	0.0	0.7
138	-	0.0	0.0	0.0
140	-	0.0	0.0	0.0
142	-	0.1	0.2	0.0
144	5.9	5.8	4.6	2.0
146	-	0.0	0.0	0.0
148	2.8	2.5	2.7	2.8
150	-	0.5	0.7	0.0
152	13.9	13.4	10.6	4.6
154	-	0.0	0.0	0.0
158	-	0.3	0.4	0.0
160	-	0.0	0.1	0.2
162	-	0.0	0.0	0.0
164	-	0.0	0.0	0.0

Table III.2 (Continued)

Observed and Calculated Intensities of Allowable Lines in Nd-Yb Gallium Garnet (a = 12.864Å)

		I_{calc} for Postulated Structural Formulae		
$h^2+k^2+\ell^2$	I_{obs}	$\{Nd_{2.7}Yb_{0.3}\}[Yb_2](Ga_3)O_{12}$	$\{Nd_{0.7}Yb_{2.3}\}[Nd_2](Ga_3)O_{12}$	$\{Nd_{2.7}Yb_{0.3}\}[Ga_2](Yb_2Ga)O_{12}$
166	-	0.8	0.7	0.1
168	-	0.5	0.1	0.3
170	-	0.0	0.0	0.0
174	-	0.4	0.6	0.0
176	0.8	0.8	1.5	7.0
178	-	0.0	0.0	0.0
180	7.1	6.6	7.1	7.2
182	-	0.5	0.7	0.0
184	7.3	6.8	5.3	2.3
186	-	0.0	0.0	0.0
190	-	0.1	0.2	0.0
192	3.8	3.5	3.2	2.1
194	-	0.0	0.0	0.0
196	-	0.0	0.0	0.0
198	-	0.3	0.4	0.0
200	-	0.7	0.1	0.2
202	-	0.0	0.0	0.0
206	-	0.7	1.0	0.0
208	2.7	3.3	2.6	1.1
210	-	0.0	0.0	0.0
212	6.3	5.9	6.4	6.5
214	-	0.1	0.2	0.0
216	13.9	14.7	11.6	5.1
218	-	0.0	0.0	0.0
222	-	0.4	0.5	0.0
224	-	0.4	0.1	0.4
226	-	0.0	0.0	0.0
230	-	0.9	1.2	0.0
232	-	0.2	0.0	0.2
234	-	0.0	0.0	0.0
236	-	0.0	0.0	0.0

Table III.2 (Continued)

Observed and Calculated Intensities of Allowable Lines in Nd-Yb Gallium Garnet (a = 12.86$_4$Å)

		I_{calc} for Postulated Structural Formulae		
$h^2+k^2+\ell^2$	I_{obs}	$\{Nd_{2.7}Yb_{0.3}\}[Yb_2](Ga_3)O_{12}$	$\{Nd_{0.7}Yb_{2.3}\}[Nd_2](Ga_3)O_{12}$	$\{Nd_{2.7}Yb_{0.3}\}[Ga_2](Yb_2Ga)O_{12}$
238	-	0.0	0.5	0.0
242	-	0.0	0.0	0.0
244	5.6	6.7	7.3	7.5
246	-	0.4	0.6	0.0
248	17.5	16.7	13.1	5.6
250	-	0.0	0.0	0.0
R-factor (%):		9.6	19.3	50.1

$$R = \frac{\sum(|I_{obs}-I_{calc}|)}{\sum I_{obs}} \times 100$$

Table III.3

Observed and Calculated Intensities of Allowable Lines in Pr-Lu Gallium Garnet (a = 12.94$_2$Å)

$h^2+k^2+\ell^2$	I_{obs}	I_{calc} for Postulated Structural Formulae		
		$\{Pr_3\}[Lu_2](Ga_3)O_{12}$	$\{PrLu_2\}[Pr_2](Ga_3)O_{12}$	$\{Pr_3\}[Ga_2](Lu_2Ga)O_{12}$
6	8.3	11.7	18.0	0.0
8	9.7	19.7	4.0	7.4
14	6.2	6.1	10.1	0.0
16	57.5	60.2	48.1	22.2
20	88.1	89.5	100	100
22	-	0.1	0.5	0.9
24	100	100	77.8	33.0
26	1.2	1.1	1.0	0.7
30	8.0	7.0	9.1	0.6
32	1.1	1.1	0.0	2.7
38	7.8	6.9	9.1	0.6
40	4.7	5.9	0.0	0.0
42	-	0.0	0.0	0.0
46	1.7	0.9	1.6	0.0
48	4.1	4.5	8.1	15.0
50	-	0.0	0.0	0.0
52	30.6	24.0	26.5	25.7
54	2.1	2.6	3.5	0.1
56	76.9	64.4	50.8	23.1
62	1.5	1.4	2.2	0.1
64	20.3	18.0	16.6	11.3
66	-	0.1	0.1	0.1
68	-	0.1	0.1	0.0
70	-	0.3	0.6	0.0
72	2.3	2.2	0.4	1.0
74	-	0.0	0.0	0.0

Table III.3 (Continued)

Observed and Calculated Intensities of Allowable Lines in Pr-Lu Gallium Garnet (a = 12.942Å)

		I_{calc} for Postulated Structural Formulae		
$h^2+k^2+\ell^2$	I_{obs}	$\{Pr_3\}[Lu_2](Ga_3)O_{12}$	$\{PrLu_2\}[Pr_2](Ga_3)O_{12}$	$\{Pr_3\}[Ga_2](Lu_2Ga)O_{12}$
78	-	0.4	0.6	0.0
80	17.0	15.5	12.1	5.4
84	17.4	14.1	16.0	16.3
86	0.9	1.0	1.6	0.1
88	12.5	12.6	9.9	4.4
90	-	0.2	0.1	0.1
94	0.9	0.8	1.2	0.0
96	0.9	0.9	0.2	0.3
98	-	0.2	0.2	0.2
100	-	0.0	0.0	0.0
102	-	0.2	0.4	0.0
104	1.4	1.3	0.1	0.7
106	-	0.0	0.0	0.0
110	1.6	1.1	1.6	0.0
114	-	0.0	0.0	0.0
116	11.8	11.7	13.2	13.4
118	-	0.5	0.7	0.0
120	16.4	13.2	10.4	4.6
122	-	0.0	0.0	0.0
126	-	0.9	1.3	0.0
128	9.7	8.6	8.0	5.4
134	0.6	0.6	0.7	0.0
136	-	0.5	0.0	0.6
138	-	0.0	0.0	0.0
140	-	0.0	0.0	0.0
142	-	0.2	0.4	0.0

Table III.3 (Continued)

Observed and Calculated Intensities of Allowable Lines in Pr-Lu Gallium Garnet (a = 12.942Å)

		I_{calc} for Postulated Structural Formulae		
$h^2+k^2+\ell^2$	I_{obs}	$\{Pr_3\}[Lu_2](Ga_3)O_{12}$	$\{PrLu_2\}[Pr_2](Ga_3)O_{12}$	$\{Pr_3\}[Ga_2](Lu_2Ga)O_{12}$
144	6.5	5.8	4.6	2.0
146	-	0.0	0.0	0.0
148	2.3	2.4	2.7	2.8
150	-	0.5	0.7	0.0
152	13.2	13.4	10.4	4.6
154	-	0.0	0.0	0.0
158	-	0.3	0.4	0.0
160	-	0.3	0.0	0.2
162	-	0.0	0.0	0.0
164	-	0.0	0.0	0.0
166	0.8	0.7	0.9	0.0
168	-	0.5	0.0	0.3
170	-	0.0	0.0	0.0
174	-	0.4	0.6	0.0
176	1.3	0.7	1.6	3.5
178	-	0.0	0.0	0.0
180	5.6	6.3	7.2	7.2
182	-	0.5	0.7	0.0
184	6.5	6.8	5.3	2.3
186	-	0.0	0.0	0.0
190	-	0.1	0.2	0.0
192	4.0	3.4	3.2	2.2
194	-	0.0	0.0	0.0
196	-	0.0	0.0	0.0
198	-	0.2	0.4	0.0
200	0.9	1.0	0.1	0.5

Table III.3 (Continued)

Observed and Calculated Intensities of Allowable Lines in Pr-Lu Gallium Garnet (a = 12.94$_2$Å)

		I_{calc} for Postulated Structural Formulae		
$h^2+k^2+\ell^2$	I_{obs}	$\{Pr_3\}[Lu_2](Ga_3)O_{12}$	$\{PrLu_2\}[Pr_2](Ga_3)O_{12}$	$\{Pr_3\}[Ga_2](Lu_2Ga)O_{12}$
202	-	0.0	0.0	0.0
206	0.7	0.6	1.0	0.0
208	3.2	3.3	2.5	1.1
210	-	0.0	0.0	0.0
212	5.8	5.6	8.6	6.5
214	-	0.1	0.2	0.0
216	14.7	14.8	11.5	5.1
218	-	0.0	0.0	0.0
222	-	0.3	0.5	0.0
224	-	0.4	0.0	0.4
226	-	0.0	0.0	0.0
230	0.8	0.8	1.1	0.0
232	-	0.2	0.0	0.2
234	-	0.0	0.0	0.0
236	-	0.0	0.0	0.0
238	-	0.3	0.5	0.0
242	-	0.0	0.0	0.0
244	6.5	6.4	9.7	7.6
246	-	0.4	0.6	0.0
248	17.6	17.2	13.2	5.8
250	-	0.0	0.0	0.0
R-factor (%):		9.7	27.5	54.5

Table III.4

Observed and Calculated Intensities of Nine Key Lines in Nd-Yb Gallium Garnet ($a = 12.86_4$ Å)

		I_{calc} for Postulated Structural Formulae with Indicated Values of w in $\{Nd_{2.7-w}Yb_{0.3+w}\}[Nd_wYb_{2-w}](Ga_3)O_{12}$				
$h^2+k^2+\ell^2$	I_{obs}	w = 0	0.5	1.0	1.5	2.0
20	97.7	94.0	100	100	100	100
24	100	100	94.9	91.2	78.4	78.4
52	27.0	25.2	26.7	26.6	24.7	26.4
56	68.6	64.4	63.9	59.5	51.4	51.7
80	15.9	15.5	14.8	14.2	12.2	12.3
84	16.6	15.0	16.0	16.0	14.9	16.1
88	12.2	12.3	12.5	11.6	10.0	10.1
116	13.3	12.3	13.1	13.1	12.2	13.2
120	13.6	13.3	12.6	12.1	10.5	10.5
R'-factor (%):		3.5	4.3	6.9	15.1	14.0

For definition of R', see text of dissertation (p. 40)

Table III.5

Observed and Calculated Intensities of Nine Key Lines in Pr-Lu Gallium Garnet (a = 12.94$_2$Å)

		I_{calc} for Postulated Structural Formulae with Indicated Values of w in $\{Pr_{3-w}Lu_w\}[Pr_wLu_{2-w}](Ga_3)O_{12}$					
$h^2+k^2+\ell^2$	I_{obs}	w = 0	0.3	0.5	1.0	1.5	2.0
20	88.1	89.5	94.5	98.0	100	100	100
24	100	100	100	100	93.2	85.1	77.8
52	30.6	24.0	25.3	26.2	26.7	26.6	26.5
56	76.9	64.4	64.6	64.6	60.4	55.4	50.8
80	17.0	15.5	15.5	15.5	14.4	13.2	12.1
84	17.4	14.4	14.9	15.5	15.9	16.0	16.0
88	12.5	12.6	12.7	12.7	11.8	10.8	9.9
116	11.8	11.7	12.5	13.8	13.1	13.7	13.2
120	16.4	13.2	13.3	13.3	12.4	11.3	10.4
R' (%):		7.7	8.6	9.5	13.4	17.9	21.7

IV. GARNET PREPARATIONS

Iron garnet systems have received great attention in the recent past, and considerable attention at the present time as bubble domain materials and for use in optical waveguides (47). Most iron-containing systems have been studied from various aspects, mainly with regard to their magnetic properties since the discovery of ferrimagnetic interaction between ferric ions in octahedral and tetrahedral sites in YIG (9, 10). Geller et al. (48) were able to prepare $\{GdCa_2\}[Zr_2](Fe_3)O_{12}$ garnet.

Loriers and his co-workers (49) studied the system $\{Gd_3\}-[Sc_xFe_{2-x}](Fe_3)O_{12}$ and $\{Nd_3\}[Sc_xFe_{2-x}](Fe_3)O_{12}$, but they were not able to prepare compounds with the octahedral sites filled with Sc^{3+} (i.e., x=2) completely. Preparations of the type $\{RE_3\}[Sc_xFe_{2-x}](Fe_3)O_{12}$ were studied by Mill (50), but he was not able to fill the octahedral sites with Sc^{3+} completely. The results of Mill's work are compiled in Table IV.1. Geller et al. (54) studied the systems $\{Y_3\}[Sc_xFe_{2-x}](Fe_x)O_{12}$ and $\{Y_{3-y}Ca_y\}[Fe_{2-x}Sc_x](Fe_{3-y}Si_y)O_{12}$. The maximum value of x was 1.50 in the $\{Y_3\}[Sc_xFe_{2-x}](Fe_3)O_{12}$ system and 1.10 in the $\{Y_{3-y}Ca_y\}[Fe_{2-x}Sc_x](Fe_{3-y}Si_y)O_{12}$ system. A number of compounds of the general formula $\{RE_3\}[Sc_2](Al_3)O_{12}$ were prepared by Kokta (52). Single phase garnet resulted only when the RE was Sm or Eu.

In all the papers (Ref. 47-52) discussed Sc^{3+} does not exist in dodecahedral sites. Loriers et al. (49) made

Table IV.1 From Reference 50.

Composition	Molecular Ratio of $RE_2O_3:Sc_2O_3:Fe_2O_3$	a_{max} (Å)	$x_{max.}$
$Nd_3Fe_{5-x}Sc_xO_{12}$	3:2:3	garnet not formed	
	3:1.75:3.25	12.707	1.32
	3:0.75:4.25	12.673	0.90
$Sm_3Fe_{5-x}Sc_xO_{12}$	3:0.50:4.50	little garnet	
	3:2.2:3	12.663	1.66
	3:2.2:2.8	12.664	1.67
	3:2:3	12.663	1.66
$Gd_3Fe_{5-x}Sc_xO_{12}$	3:2.2:3	12.606	1.67
	3:2.2:2.8	12.606	1.67
	3:2:3	12.605	1.66
$Tb_3Fe_{5-x}Sc_xO_{12}$	3:2.2:3	12.570	1.65
$Er_3Fe_{5-x}Sc_xO_{12}$	3:2:3	little garnet	
	3:1.85:3.15	12.450	1.26
	3:1.75:3.25	12.450	1.26
	3:1.5:3.5	12.451	1.27
$Yb_3Fe_{5-x}Sc_xO_{12}$	3:1:4	little garnet	
	3:0.85:4.15	12.342	0.50
	3:0.75:4.25	12.342	0.50

preparation in the system $\{Nd_{3-y}Sc_y\}[Fe_{2-x}Sc_x](Fe_3)O_{12}$ with the small value of y but they were not able to prepare the garnet with x=2. Kokta (53) studied the preparation of $\{RE_{3-y}Sc_y\}[Sc_2](Fe_3)O_{12}$, where RE is Nd, Sm, Eu, Gd, Tb, Dy, Ho, Er, Tm, Yb, or Lu. The present work dealing with this dissertation is the continuation of work on this system.

In the present work, exploratory experiments indicated that the garnets with minimum y claimed by Kokta are not single-phase garnets. In the present work detailed studies were carried out and the minimum and maximum values of y were sought. The investigation on magnetic properties of such compounds offer the possibility of direct c-d interactions in the absence of magnetic a-site ions.

Gilleo and Geller (54) observed ferrimagnetism at very low temperature in $\{Gd_3^{3+}\}[Mn_2^{2+}](GaGe_2)O_{12}$. This shows that a dodecahedral-octahedral superexchange interaction is possible between a rare earth ion and a transition metal ion even in the absence of magnetic ions on the tetrahedral sites. In this direction to seek such a dodecahedral-octahedral interaction between rare earth and ferric ions the hypothetical compounds such as $\{RE_3^{3+}\}[Fe_2^{3+}](Be_2^{2+}V^{5+})O_{12}$, $\{RE_3^{3+}\}[Fe_2^{3+}](Li^{+}Si_2^{4+})O_{12}$, and $\{RE_3^{3+}\}[Fe_2^{3+}](Li^{+}Ge_2^{4+})O_{12}$ were studied.

Another possible rare earth-Fe interaction considered in this project was the system in which the magnetic rare earth ion (e.g., Yb^{3+}) is on the octahedral site, the ferric ion is on the tetrahedral site and the dodecahedral site contains nonmagnetic ions. Attempts were made to study the systems $\{Sr_{3-x}La_x\}[Yb_2](Ge_{3-x}Fe_x)O_{12}$, $\{Ca_{3-x}La_x\}[Yb_2](Ge_{3-x}Fe_x)O_{12}$, and $\{Ca_3\}[Yb_2](Fe_xGe_{3-x})O_{12-x}F_x$ in order to investigate this possible rare earth-Fe interaction.

A summary of all the attempts which have been made to study the crystal chemistry and magnetic properties of new garnets studied in this doctoral project is:

(1) $\{RE_{3-y}Sc_y\}[Sc_2](Fe_3)O_{12}$, $\{Nd_3\}[Sc_2](Fe_zGa_{3-z})O_{12}$, and $\{Nd_{3-(w+y)}M_wSc_y\}[Sc_2](Fe_3)O_{12}$.

(2) $\{Pr_{3-y}Lu_y\}[Lu_xGa_{2-x}](Ga_3)O_{12}$.

(3) $\{Nd_{2.8}Yb_{0.2}\}[Yb_2](Ga_{3-z}Fe_z)O_{12}$.

(4) $\{Nd_{2.8}Lu_{0.2}\}[Lu_2](Ga_{3-z}Fe_z)O_{12}$.

(5) $\{Nd_3\}[Lu_2](Fe_zGa_{3-z})O_{12}$.

(6) $\{Pr_3\}[Lu_2](Fe_zGa_{3-z})O_{12}$.

(7) $\{Sr_{3-x}La_x\}[Yb_2](Ge_{3-x}Fe_x)O_{12}$.

(8) $\{RE_3\}[Fe_2](LiSi_2)O_{12}$ and $\{RE_3\}[Fe_2](Ge_2Li)O_{12}$.

(9) $\{RE_3\}[Fe_2](VBe_2)O_{12}$.

(10) $\{Sr_3\}[Lu_2](Fe_xGe_{3-x})O_{12-x}F_x$.

(11) $\{Ca_3\}[Lu_2](Fe_xGe_{3-x})O_{12-x}F_x$.

(12) $\{RE_{1+y}Ca_{2-y}\}[Zr_{2-x/2}Ca_{x/2}](Fe_3)O_{12}$.

(13) $\{BiY_2\}[RE_2](Fe_3)O_{12}$.

These systems will be explained in detail later.

IV.1.1 Neodymium-Scandium-Iron System. Attempts to prepare the compound $\{Nd_3\}[Sc_2](Fe_3)O_{12}$ have been unsuccessful (49, 50) up to now, and it is also very well known that even $\{Nd_3\}[Fe_2](Fe_3)O_{12}$ garnet does not exist.

The ionic radius of Nd^{3+} (55) is so large that it prohibits the formation of the pure garnet, $\{Nd_3\}[Sc_2](Fe_3)O_{12}$. It was suggested the possibility that pure phases would be found in compositions $\{Nd_{3-y}Sc_y\}[Sc_2](Fe_3)O_{12}$. This attempt failed (Table IV.2).

Table IV.2 System $\{Nd_{3-y}Sc_y\}[Sc_2](Fe_3)O_{12}$

y	Purity
0.0	impure
0.1	impure
0.2	impure
0.25	impure
0.30	slightly impure
0.35	slightly impure

Table IV.2 (Continued)

y	Purity
0.40	impure
0.50	impure
0.70	impure
0.80	impure
1.00	impure
1.20-3.00	impure

Direction of increasing purity

Because of the failure of the above mentioned approach, different procedures were tried.

A. It was postulated that in order to prepare single phase Nd garnets with iron in tetrahedral sites the average ionic radius of the tetrahedral site should be decreased by introducing ions smaller than Fe^{3+} ions. Therefore, the $\{Nd_3\}[Sc_2](Fe_zGa_{3-z})O_{12}$ system was studied. The results are compiled in Table IV.3 and plotted in Fig. IV.1.

Table IV.3 System $\{Nd_3\}[Sc_2](Fe_zGa_{3-z})O_{12}$

z	Purity	a(Å)
0.0	Pure	12.657
0.2	Pure	12.664
0.6	Pure	12.674
0.8	Pure	12.683
1.2	Pure	12.694
1.8	Pure	12.712
2.2	Pure	12.727
2.4	Pure	12.735
2.6	Pure	12.740
2.7	Slightly impure	12.740
2.8-3.0	Impure	-

Fig. IV.1

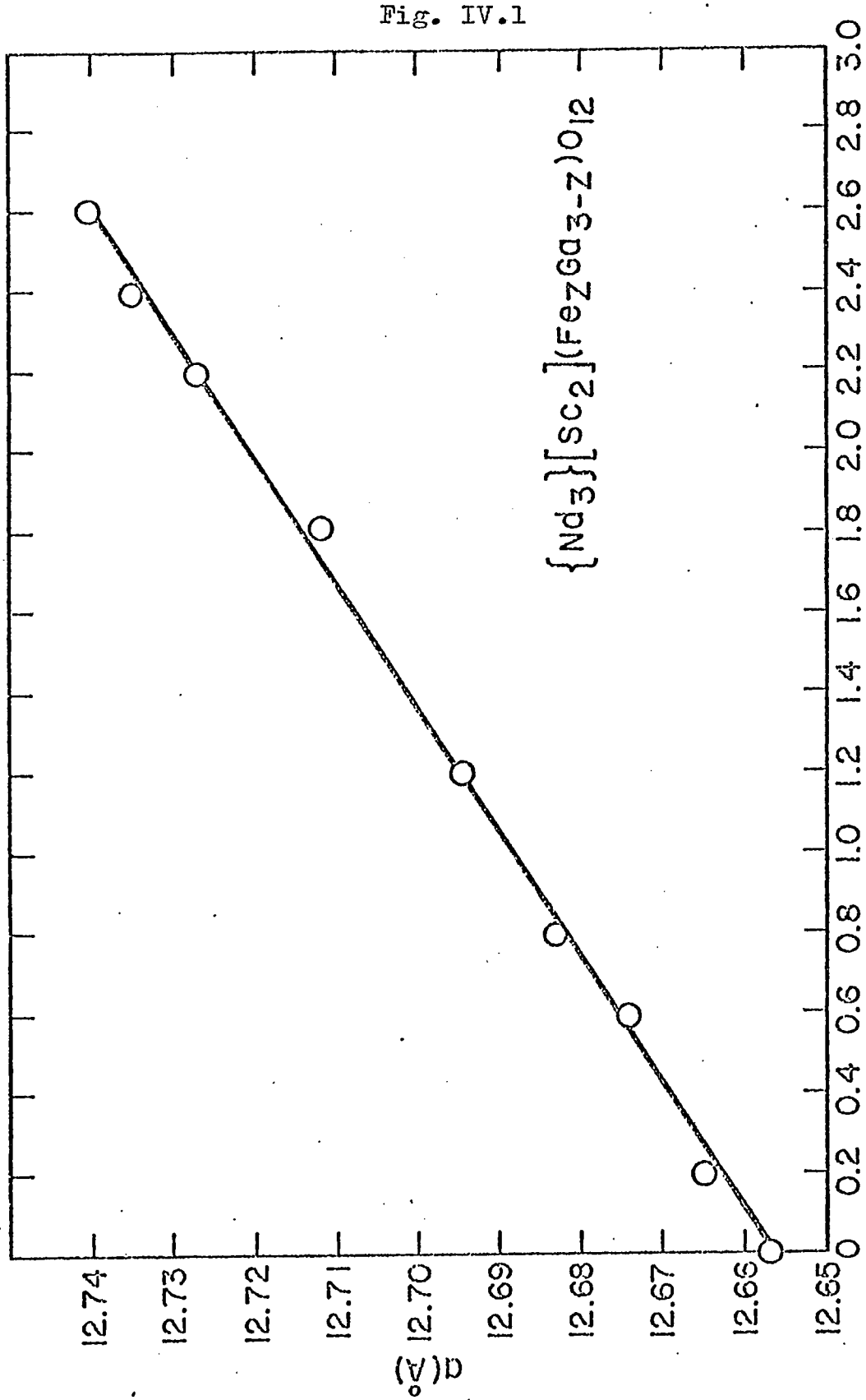

Lattice constant versus z in $\{Nd_3\}[Sc_2](Fe_zGa_{3-z})O_{12}$

B. The failure to obtain single phase garnet compositions in $\{Nd_{3-y}Sc_y\}[Sc_2](Fe_3)O_{12}$ suggested another approach. It was postulated that in order to prepare single phase Nd garnet with iron in tetrahedral sites a small amount of ions with larger ionic radius than Sc^{3+} should be introduced in the c-sites along with Nd. Therefore, the systems $\{Nd_{3-(w+y)}M_wSc\}[Sc_2](Fe_3)O_{12}$, where M is Gd, Y, or Lu were studied. The results are compiled in Table IV.4.

Table IV.4 $\{Nd_{3-(w+y)}M_wSc_y\}[Sc_2](Fe_3)O_{12}$

		M=Gd	
w	y	Purity	a(Å)
0.1	0.0	Impure	-
0.1	0.1	Impure	-
0.1	0.2	Slightly impure	-
0.1	0.3	Pure	12.711
0.1	0.4	Slightly impure	-
0.1	0.5	Impure	-
0.2	0.1	Impure	-
0.2	0.2	Slightly impure	-
0.2	0.3	Pure	12.708
0.2	0.4	Impure	-
0.3	0.1	Impure	-
0.3	0.2	Slightly impure	-
0.3	0.3	Pure	12.704
0.3	0.4	Slightly impure	-
0.4	0.1	Impure	-
0.4	0.2	Slightly impure	-
0.4	0.3	Pure	12.699
0.4	0.4	Slightly impure	-

Table IV.4 (Continued)

w	y	Purity	a(Å)
		M=Y	
0.1	0.0	Impure	-
0.1	0.1	Impure	-
0.1	0.2	Impure	-
0.1	0.3	Impure	-
0.2	0.0	Impure	-
0.2	0.1	Impure	-
0.2	0.2	Impure	-
0.2	0.3	Impure	-
0.2	0.4	Impure	-
0.3	0.0	Impure	-
0.3	0.1	Impure	-
0.3	0.2	Impure	-
0.3	0.3	Impure	-
0.3	0.4	Impure	-
0.4	0.0	Impure	-
0.4	0.1	Slightly impure	-
0.4	0.2	Pure	12.707
0.4	0.3	Slightly impure	-
0.4	0.4	Impure	-
0.5	0.0	Impure	-
0.6	0.0	Impure	-
		M=Lu	
0.1	0.0	Impure	-
0.1	0.1	Impure	-
0.1	0.2	Impure	-
0.1	0.3	Impure	-

Table IV.4 (Continued)

w	y	M=Lu Purity	a(Å)
0.2	0.1	Impure	-
0.2	0.2	Impure	-
0.2	0.3	Impure	-
0.2	0.4	Impure	-
0.3	0.1	Impure	-
0.3	0.2	Impure	-
0.3	0.3	Slightly impure	-
0.3	0.4	Pure	12.698
0.4	0.1	Impure	-
0.4	0.2	Slightly impure	-
0.4	0.3	Pure	12.694
0.4	0.4	Pure	12.691

IV.2.1 Attempts to prepare Pr-Sc-Iron garnets. Substitution was attempted in the nominal formula $\{Pr_{3-y}Sc_y\}[Sc_2](Fe_zGa_{3-z})O_{12}$.

IV.2.2 Results. An attempt to determine the y-value in this system was made. Runs were made with z=0 and the y-value was increased up to 3.0. It was found that no single phase resulted. Attempts were also made to get single-phase materials with different values of z but this system was not studied in detail (i.e. it was tried for z=1.6-3.0). The two attempts failed.

IV.3.1 Related compounds of general formula $\{R_{3-y}Sc_y\}[Sc_2](Fe_3)O_{12}$. Attempts were made to determine minimum and maximum values of y required to yield a single-phase in the system $\{R_{3-y}Sc_y\}[Sc_2](Fe_3)O_{12}$ where R is Sm, Eu, Gd, Tb, Dy, Ho, Er, Tm, Yb or Lu. The resulting compounds are listed in Table IV.5 and they are shown graphically in Figs. IV.2 and IV.3.

Table IV.5

$\{Sm_{3-y}Sc_y\}[Sc_2](Fe_3)O_{12}$		
y	Purity	a(Å)
0.0	Pure	12.664
0.1	Pure	12.660
0.2	Pure	12.656
0.3	Pure	12.652
0.4	Pure	12.650
0.5	Pure	12.646
0.6	Pure	12.640
0.7	Pure	12.363

Table IV.5 (Continued)

y	Purity	a(Å)
0.8	Pure	12.634
0.9	Pure	12.630
1.0-3.0	Impure	-
$\{Eu_{3-y}Sc_y\}[Sc_2](Fe_3)O_{12}$		
0.0	Pure	12.637
0.1	Pure	12.635
0.2	Pure	12.632
0.4	Pure	12.621
0.6	Pure	12.616
0.7	Pure	12.610
0.8-3.0	Impure	-
$\{Gd_{3-y}Sc_y\}[Sc_2](Fe_3)O_{12}$		
0.0	Impure	-
0.1	Impure	-
0.15	Pure	12.611
0.20	Pure	12.608
0.25	Pure	12.605
0.30	Pure	12.603
0.40	Pure	12.598
0.50	Pure	12.593
0.60	Pure	12.586
0.7-3.0	Impure	-

Table IV.5 (Continued)

$\{Tb_{3-y}Sc_y\}[Sc_2](Fe_3)O_{12}$		
y	Purity	a(Å)
0.0-0.2	Impure	-
0.25	Pure	12.562
0.40	Pure	12.558
0.50	Pure	12.554
0.6-3.0	Impure	-
$\{Dy_{3-y}Sc_y\}[Sc_2](Fe_3)O_{12}$		
0.0-0.25	Impure	-
0.30	Pure	12.514
0.40-3.0	Impure	-

Upon attempting to prepare $\{R_{3-y}Sc_y\}[Sc_2](Fe_3)O_{12}$ compounds with the small trivalent rare earth ion, R, being Ho^{3+}, Er^{3+} and Tm^{3+} it was found that garnets were formed in all cases but with additional phases present. In the cases where R is Yb^{3+} or Lu^{3+} garnet phases were not observed at all.

IV.3.2 Discussion of Results. The resulting compounds of system $\{R_{3-y}Sc_y\}[Sc_2](Fe_3)O_{12}$ where R is Sm, Eu, Gd or Dy are listed in Table IV.5 and they are shown graphically in Figs. IV.2, IV.3, IV.4 and IV.5.

Fig. IV.3 illustrates the relationship between the maximum and minimum compositions and the Shannon-Prewitt (55)

radii of the trivalent rare earths. Fig. IV.2 shows that in Sm and Eu preparations the y-value is zero. This figure also illustrates that in Gd and Tb preparations, the compositional limits are found to grow narrower, and finally, with Dy, only one composition occurs phase-pure. In Fig. IV.4, the difference between the maximum and minimum y values (Δy) are plotted vs the rare earth radii to illustrate that this relationship is also more or less regular. Fig. IV.5, illustrates the relationship between the average dodecahedral ion radius of the maximum and minimum composition and the Shannon-Prewitt (55) radii of trivalent rare earth ions.

It is to be noted in Table IV.5 that on going along the rare earth series from the larger ions to the smaller one the minimum value of y increases. The increase in the y value means a decrease of the average ionic radius of the dodecahedral sites (the ionic radius of Sc^{3+} (Table IV.6) is smaller than those of trivalent rare earth ions). From these values one would certainly expect to have a single phase when R is Ho^{3+}, Er^{3+}, Tm^{3+}, Yb^{3+} or Lu^{3+} with increasing value of y. This trend is rather unexpected and one would expect just the opposite result because it was shown (Table I.4) that the existence of rare earth iron garnets is limited to certain rare earth ionic radii. In other words, it is possible to prepare iron garnets of all the rare earth ions from Sm^{3+} to Lu^{3+} but it is impossible to prepare garnets containing only large rare earth ions such as Pr^{3+} and Nd^{3+} on the dodecahedral sites. The reason that preparation of small rare earth (Ho,

Fig. IV.2

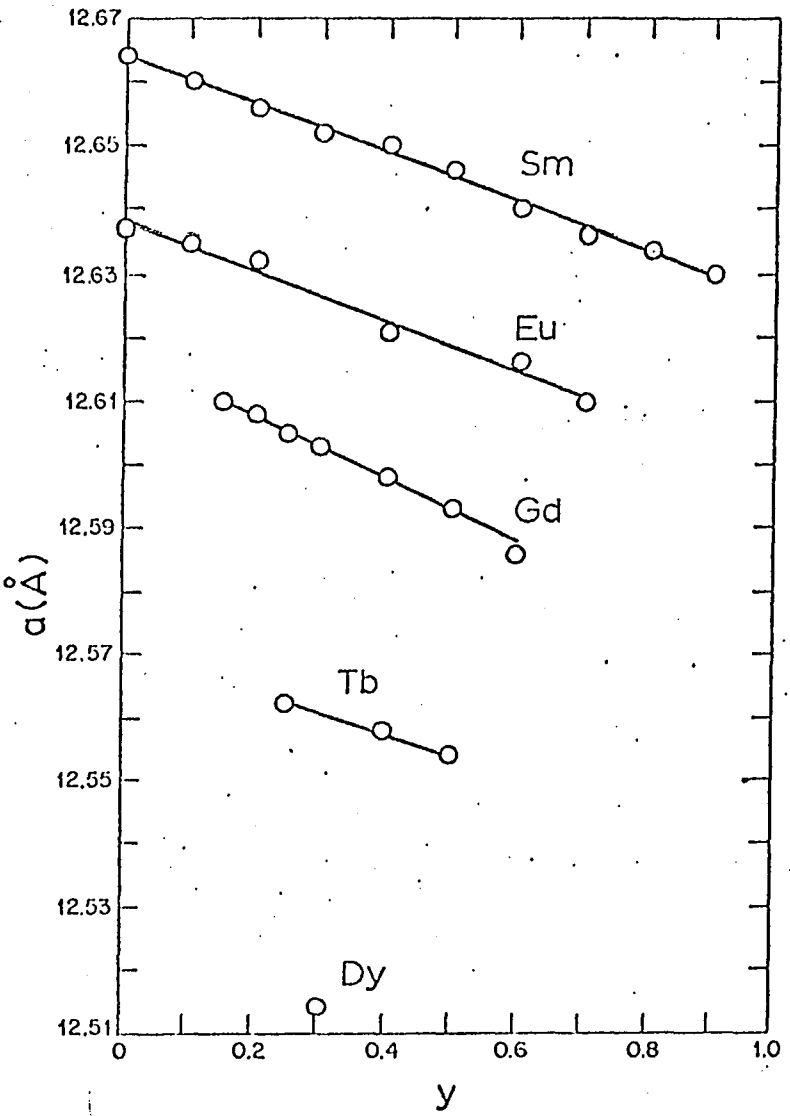

Lattice constants vs. composition (in terms of y) in $\{RE_{3-y}Sc_y\}[Sc_2](Fe_3)O_{12}$, where RE is identified in each case.

Fig. IV.3

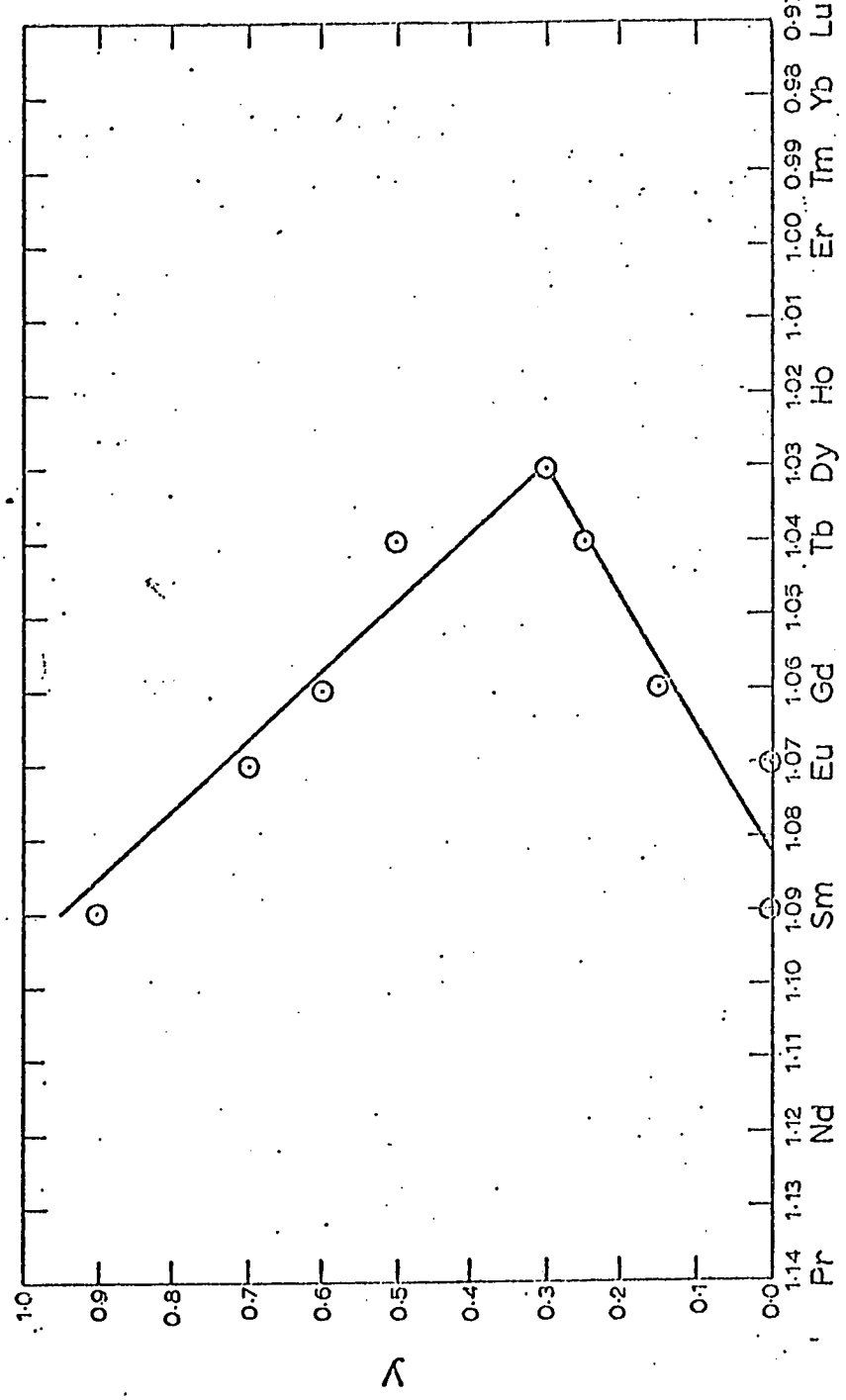

Relationship between rare earth radius and maximum and minimum y-values in $\{RE_{3-y}Sc_y\}[Sc_2](Fe_3)O_{12}$

Fig. IV.4

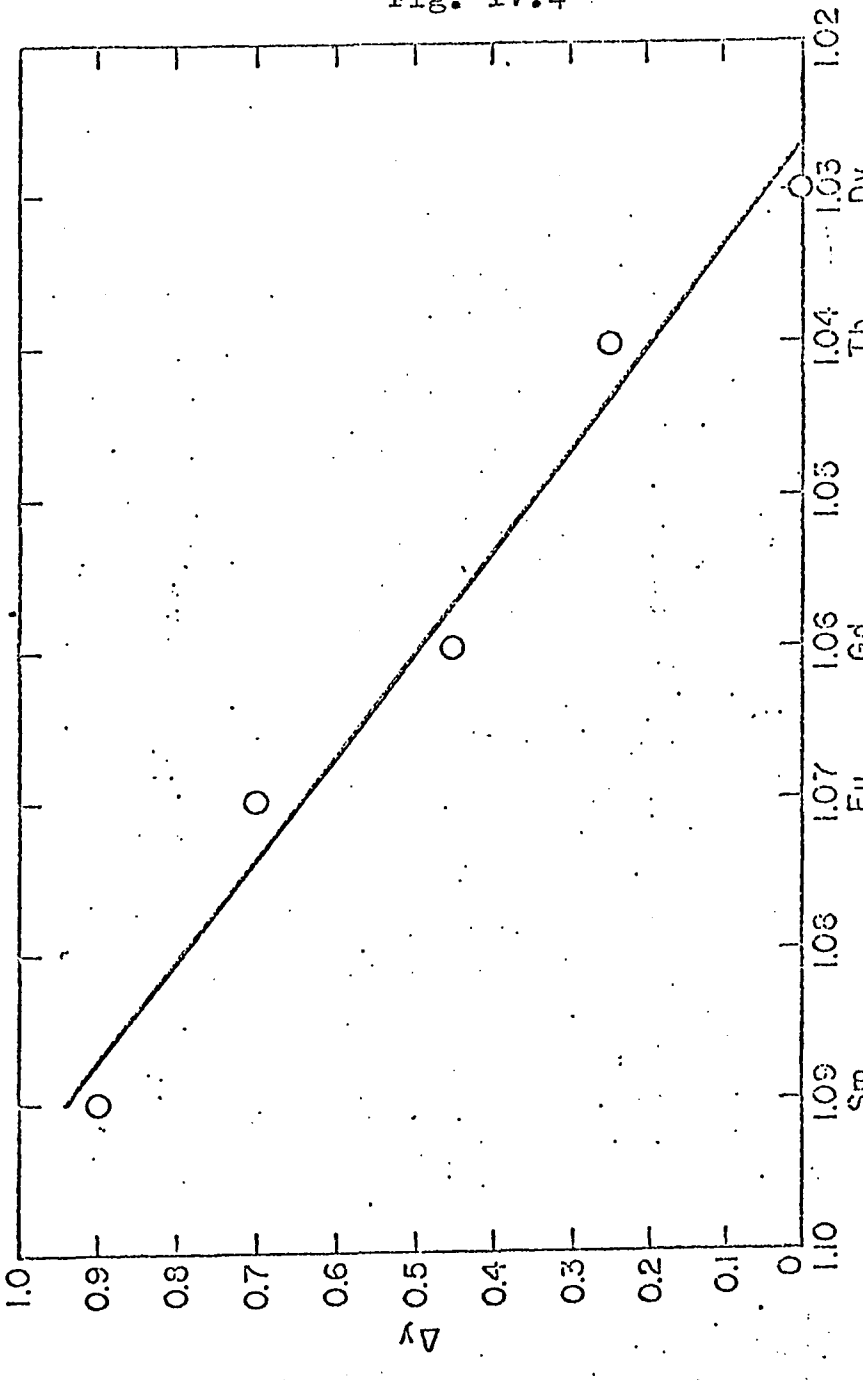

Relationship between rare earth radius and Δy (i.e., $y_{max} - y_{min}$) in $\{RE_{3-y}Sc_y\}[Sc_2](Fe_3)O_{12}$

Er, Tm, Yb and Lu)-scandium-Fe garnets is impossible might suggest that some of the small rare earth ion enters the octahedral sites, thereby pushing some of the Sc^{3+} out and resulting in a second phase.

If we suggest that the small rare earth ions (that is, Ho, Er, Tm, Yb and Lu) do not enter octahedral sites then one may question why $\{Ho_3\}[Sc_2](Fe_3)O_{12}$ does not form because the ionic radii of Ho^{3+} (see Table IV.6) is more than the average dodecahedral ion radius of single phase $\{Dy_{2.7}Sc_{0.3}\}[Sc_2](Fe_3)O_{12}$ (that is, 1.01_4 Å). This question possibly could be answered by considering the relative ionic sizes of the rare earth and scandium in dodecahedral sites. For smaller rare earths the tendency for scandium to join it in the dodecahedral sites increases and i theoretical composition results (when Sc also fills all the octahedral sites) in which the average ion radius is too small for the garnet structure to remain stable.

Table IV.6 Ionic radius of Sc^{3+}, Y^{3+}, and trivalent rare earth ions with coordination number 8 (Ref. 55).

Ion	Ionic radius (Å)
Pr^{3+}	1.14
Nd^{3+}	1.12
Sm^{3+}	1.09
Eu^{3+}	1.07
Gd^{3+}	1.06
Tb^{3+}	1.04
Dy^{3+}	1.03
Ho^{3+}	1.02
Er^{3+}	1.00

Table IV.6 (Continued)

Ion	Ionic radius (Å)
Tm^{3+}	0.99
Yb^{3+}	0.98
Lu^{3+}	0.97
Y^{3+}	1.015
Sc^{3+}	0.87

If the lower line of Fig. IV.5 (for Sc) is extrapolated to Ho^{3+} (r=1.02 Å) a minimum required y-value of about 0.38 is indicated. The average dodecahedral ion radius calculated for hypothetical $\{Ho_{2.62}Sc_{0.38}\}[Sc_2](Fe_3)O_{12}$ is 1.00_1 Å, too small to allow garnets with two Sc^{3+} ions and three Fe^{3+} ions on the octahedral and tetrahedral sites, respectively. That 1.00_1 Å is too small can be proved by analysis of data in Table IV.7. Table IV.7 gives values (calculated from data in Table IV.6) for the average dodecahedral site radii of limiting composition shown in Fig. IV.2 and listed in Table IV.5. The decrease in the maximum average dodecahedral site radius with decrease in rare earth radius is a result of an increase in minimum dodecahedral Sc content. The minimum average dodecahedral radii calculated for the materials with maximum Sc content are, on the other hand, found to give a minimum limiting value which is greater than the 1.00_1 Å value required by the hypothetical Ho composition.

Fig. IV.5

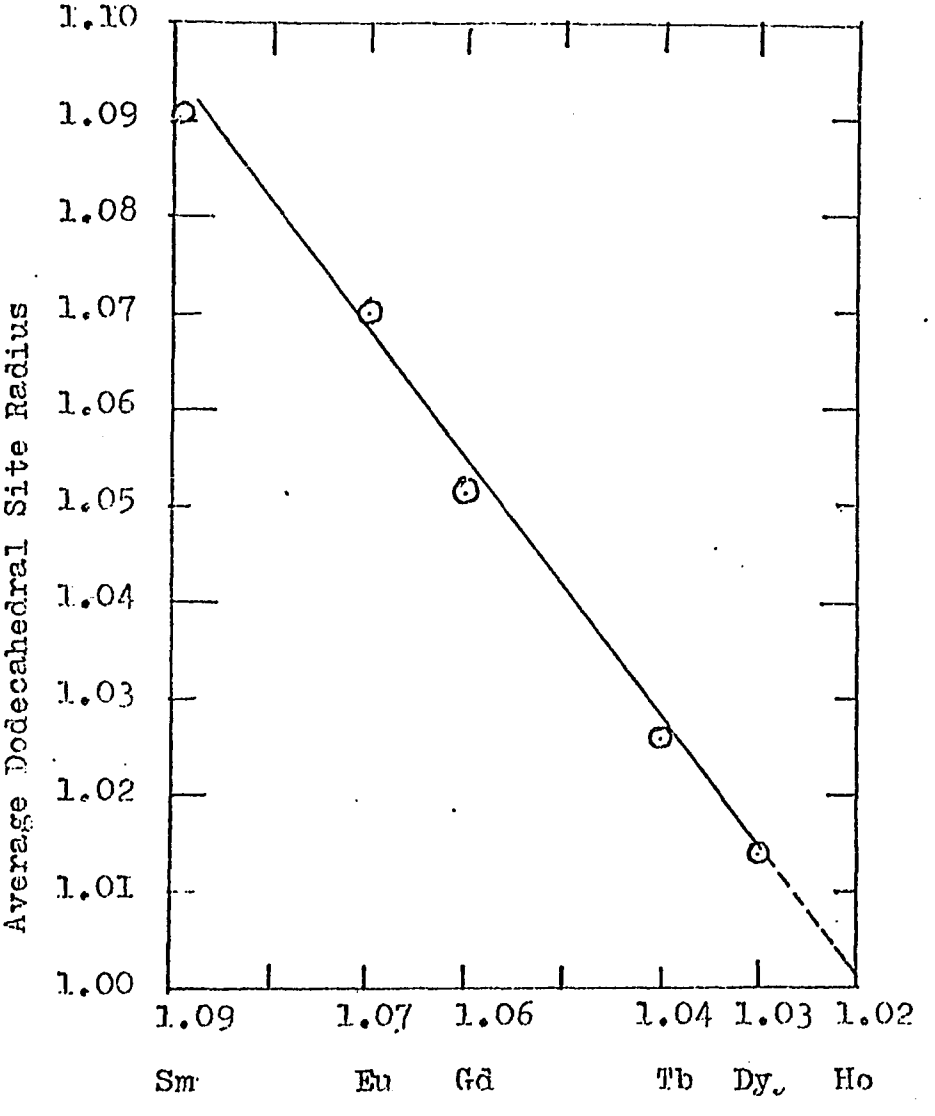

Relation between rare earth radius and average dodecahedral site radius in $\{RE_{3-y}Sc_y\}[Sc_2](Fe_3)O_{12}$

Table IV.7 Calculated average dodecahedral site radius of compounds with maximum and minimum value of y listed in Table IV.5.

$\{R_{3-y}Sc_y\}[Sc_2](Fe_3)O_{12}$	Average Dodecahedral Site Radius (Å)	
R	$y_{min.}$	$y_{max.}$
Sm	1.09	1.02_4
Eu	1.07	1.02_3
Gd	1.05_1	1.02_2
Tb	1.02_6	1.01_2
Dy	1.01_4	1.01_4

Probably $\{R_{3-y}Sc_y\}[Sc_2](Fe_3)O_{12}$ phases, where R is Nd^{3+} or Pr^{3+}, do not form because the difference between the ionic radii of Sc^{3+} and Pr^{3+} or Nd^{3+} in dodecahedral sites is too large (with Fe^{3+} filling all tetrahedral sites).

If one takes the maximum observed value of dodecahedral radius (1.09 Å, the Sm^{3+} value) and consider this value the maximum value of dodecahedral site radius for any single phase garnet, the y-value for $R=Nd^{3+}$ would have to be 0.36 which has been found to be experimentally unattainable. Such consideration suggested attempts to reduce the average radius of the ion on dodecahedral sites other than Sc^{3+} by substituting for Nd^{3+} in the system $\{Nd_{3-y}Sc_y\}[Sc_2](Fe_3)O_{12}$ small quantities of smaller rare earths (or yttrium) with, of course, then minimum required amount of Sc^{3+}. The ions so employed were

the nonmagnetic Y^{3+} and Lu^{3+} and the spin only Gd^{3+}. The result of these attempts are shown in Table IV.4.

The average dodecahedral radii of the Nd materials calculated from the radii given in Table IV.6 are given in Table IV.8. These calculations for the Nd-Y and Nd-Gd preparations appear to offer quantitative confirmation of the reasoning mentioned. In the case of the Nd-Lu material their very existence gives additional quantitative support, but their observed lattice constants and the average dodecahedral radii calculated therefrom are somewhat lower than expected, indicating some flexibility.

If, however, the average dodecahedral ion radius of a neodymium preparation is about the same as that of Sm^{3+} one would expect that the lattice constant to be very close to that of $\{Sm_3\}[Sc_2](Fe_3)O_{12}$. The data in Table IV.4 indicate that this is not exactly so. The Nd materials all have lattice constants somewhat higher than lattice constants of the Sm compound. This led to attempts to calculate lattice constants for these new materials as had been done by Suchow and Kokta for gallium garnets (39, 40). In this case, the factor $\Delta a/\Delta r_{dod}$ was obtained from the data for $\{RE_3\}[Fe_2](Fe_3)O_{12}$ compounds in Table I.4, and the factor $\Delta a/\Delta r_{oct}$ from the date for the system $\{Y_3\}[Sc_xFe_{2-x}](Fe_3)O_{12}$ (51). In order to calculate $\Delta a/\Delta r_{dod}$ the average lattice constants of the $\{RE_3\}[Fe_2](Fe_3)O_{12}$ system were plotted vs the ionic radius of RE^{3+} ions (where RE is Sm, Eu, Gd, Tb, Dy, Ho, Er, Tm, Ty and Lu). The slope of this line is $\Delta a/\Delta r_{dod}$ and it

Table IV.8 Calculated average dodecahedral site radius of single-phase compounds listed in Table IV.4.

Composition	Average Dodecahedral Site Radius (Å)
$\{Nd_{2.6}Gd_{0.1}Sc_{0.3}\}[Sc_2](Fe_3)O_{12}$	1.09_3
$\{Nd_{2.5}Gd_{0.2}Sc_{0.3}\}[Sc_2](Fe_3)O_{12}$	1.09_1
$\{Nd_{2.4}Gd_{0.3}Sc_{0.3}\}[Sc_2](Fe_3)O_{12}$	1.09_2
$\{Nd_{2.3}Gd_{0.4}Sc_{0.3}\}[Sc_2](Fe_3)O_{12}$	1.08_7
$\{Nd_{2.3}Lu_{0.3}Sc_{0.4}\}[Sc_2](Fe_3)O_{12}$	1.07_2
$\{Nd_{2.3}Lu_{0.4}Sc_{0.3}\}[Sc_2](Fe_3)O_{12}$	1.07_5
$\{Nd_{2.2}Lu_{0.4}Sc_{0.4}\}[Sc_2](Fe_3)O_{12}$	1.06_7
$\{Nd_{2.4}Y_{0.4}Sc_{0.2}\}[Sc_2](Fe_3)O_{12}$	1.08_9

calculates to be 1.61. Calculations were then made for all lattice constant compositions from

$$a_{calc} = (\text{average } r_{dod} - r_{Lu}{}^{3+})(2.19) + (\text{average } r_{oct} - r_{Fe}{}^{3+})(1.61) + a_{\{Lu_3\}[Fe_2](Fe_3)O_{12}}$$

The results, given in Table IV.9, show fair to excellent agreement for most of the materials, but the $\{Sm_3\}[Sc_2](Fe_3)O_{12}$ value is further off than one would wish. The lattice constants of the neodymium preparations are therefore justifiably high and it is the Sm compound value which is low. The reason for this apparent shrinkage is not clear; it cannot be due to site switching (that is, transfer of some rare earth to the octahedral site and, simultaneously of additional Sc to the dodecahedral site) because this would result in an even higher calculated value of a. Suchow and Kokta (56) proposed

Table IV.9 Observed and calculated lattice constants

Compounds	Lattice Constants, a(Å) Observed	Calculated
$\{Sm_3\}[Sc_2](Fe_3)O_{12}$	12.66_4	12.70_4
$\{Eu_3\}[Sc_2](Fe_3)O_{12}$	12.63_7	12.66_0
$\{Gd_{2.85}Sc_{0.15}\}[Sc_2](Fe_3)O_{12}$	12.61_1	12.61_8
$\{Tb_{2.75}Sc_{0.25}\}[Sc_2](Fe_3)O_{12}$	12.56_2	12.56_4
$\{Dy_{2.70}Sc_{0.30}\}[Sc_2](Fe_3)O_{12}$	12.51_4	12.53_7
$\{Nd_{2.4}Y_{0.4}Sc_{0.2}\}[Sc_2](Fe_3)O_{12}$	12.70_7	12.70_2
$\{Nd_{2.6}Gd_{0.1}Sc_{0.3}\}[Sc_2](Fe_3)O_{12}$	12.71_1	12.71_0
$\{Nd_{2.5}Gd_{0.2}Sc_{0.3}\}[Sc_2](Fe_3)O_{12}$	12.70_8	12.70_6
$\{Nd_{2.4}Gd_{0.3}Sc_{0.3}\}[Sc_2](Fe_3)O_{12}$	12.70_4	12.70_8
$\{Nd_{2.3}Gd_{0.4}Sc_{0.3}\}[Sc_2](Fe_3)O_{12}$	12.69_9	12.69_7
$\{Nd_{2.3}Lu_{0.3}Sc_{0.4}\}[Sc_2](Fe_3)O_{12}$	12.69_8	12.66_4
$\{Nd_{2.3}Lu_{0.4}Sc_{0.3}\}[Sc_2](Fe_3)O_{12}$	12.69_4	12.67_1
$\{Nd_{2.2}Lu_{0.4}Sc_{0.4}\}[Sc_2](Fe_3)O_{12}$	12.69_1	12.65_3
$\{Dy_{0.7}Sc_{2.3}\}[Dy_2](Fe_3)O_{12}$	12.51_4	12.57_2
$\{Nd_{2.3}Sc_{0.7}\}[Sc_{1.7}Lu_{0.3}](Fe_3)O_{12}$	12.69_3	12.67_1
$\{Nd_{2.3}Sc_{0.7}\}[Sc_{1.6}Lu_{0.4}](Fe_3)O_{12}$	12.69_5	12.68_0
$\{Nd_{2.2}Sc_{0.8}\}[Sc_{1.6}Lu_{0.4}](Fe_3)O_{12}$	12.69_1	12.66_1
$\{Sm_2Sc\}[SmSc](Fe_3)O_{12}$	12.66_4	12.71_6
$\{SmSc_2\}[Sm_2](Fe_3)O_{12}$	12.66_4	12.72_5
$\{Dy_{1.7}Sc_{1.3}\}[DySc](Fe_3)O_{12}$	12.51_4	12.55_5

that Lu^{3+} increased the solubility of Nd^{3+} in yttrium aluminum garnet single crystals by entering octahedral rather than dodecahedral sites. It is possible that some or all of the Lu^{3+} ions in the present cases also enter octahedral sites. This seems quite possible because of the rather small difference in the radii of these two ions. Calculation of the lattice constants of compositions with complete Lu^{3+} transfer (Table IV.9) shows are slightly higher than the lattice

constants of compositions without transfer of Lu^{3+} and therefore closer to experimental values, but they are still lower than the experimental values.

IV.4.1 $\{Pr_{3-y}Lu_y\}[Lu_xGa_{2-x}](Ga_3)O_{12}$ system. Suchow and Kokta (40) have studied garnets of the type $\{Pr_{3-y}R_y\}[R_xGa_{2-x}](Ga_3)O_{12}$ in which R is Yb, Tm, or Er. They found the minimum values (i.e. the minimum amounts of small rare earth on dodecahedral sites) which yield straight lines when lattice constants are plotted vs x for the systems $\{Pr_{3-y}R_y\}[R_xGa_{2-x}](Ga_3)O_{12}$ to be 0.5, 0.8, 1.15 for Yb, Tm and Er respectively. The y value for the case where R is Lu has not been reported.

In the present work the attempts were made to find the minimum value for the system $\{Pr_{3-y}Lu_y\}[Lu_xGa_{2-x}](Ga_3)O_{12}$.

IV.4.2 Results and Discussion. Several systems were prepared with constant y values while changing x.

It was found that, as the value of y approached 0.3, single-phase garnets were obtained. When approaching this minimum value (y=0.3) the plot of lattice constants vs x became linear. The data obtained is compiled in Table IV.10 and plotted in Fig. IV.6.

Suchow and Kokta (40) have calculated the average Shannon-Prewitt 'IR' radii for the dodecahedral site containing Pr^{3+} in the system $\{Pr_{3-y}R_y\}[R_2](Ga_3)O_{12}$ where R is Er, Tm, or Yb but they did not study the Lu system. They have compared these values with the values for the similar system $\{Nd_{3-y}R_y\}[R_2](Ga_3)O_{12}$. These values are shown in Table IV.11. It

Table IV.10

$\{Pr_{2.7}Lu_{0.3}\}[Lu_xGa_{2-x}](Ga_3)O_{12}$

x	a(Å)
0.0	12.506
0.2	12.537
0.4	12.570
0.6	12.608
0.8	12.652
1.0	12.680
1.2	12.714
1.4	12.754
1.6	12.792
1.8	12.830
2.0	12.866

will be seen that the averages involving any given small rare earth, R, are very close for Nd^{3+} and Pr^{3+}, but that the average decreases slightly as the radius of R (which also goes into octahedral positions) increases.

In the present work on this project it was found that $\{Pr_{2.7}Lu_{0.3}\}[Lu_2](Ga_3)O_{12}$ system also fits this argument (0.3 is the minimum amount of Lu^{3+} on dodecahedral sites which yields a straight line when lattice constants are plotted vs x for the system $\{Pr_{3-y}Lu_y\}[Lu_xGa_{2-x}](Ga_3)O_{12}$).

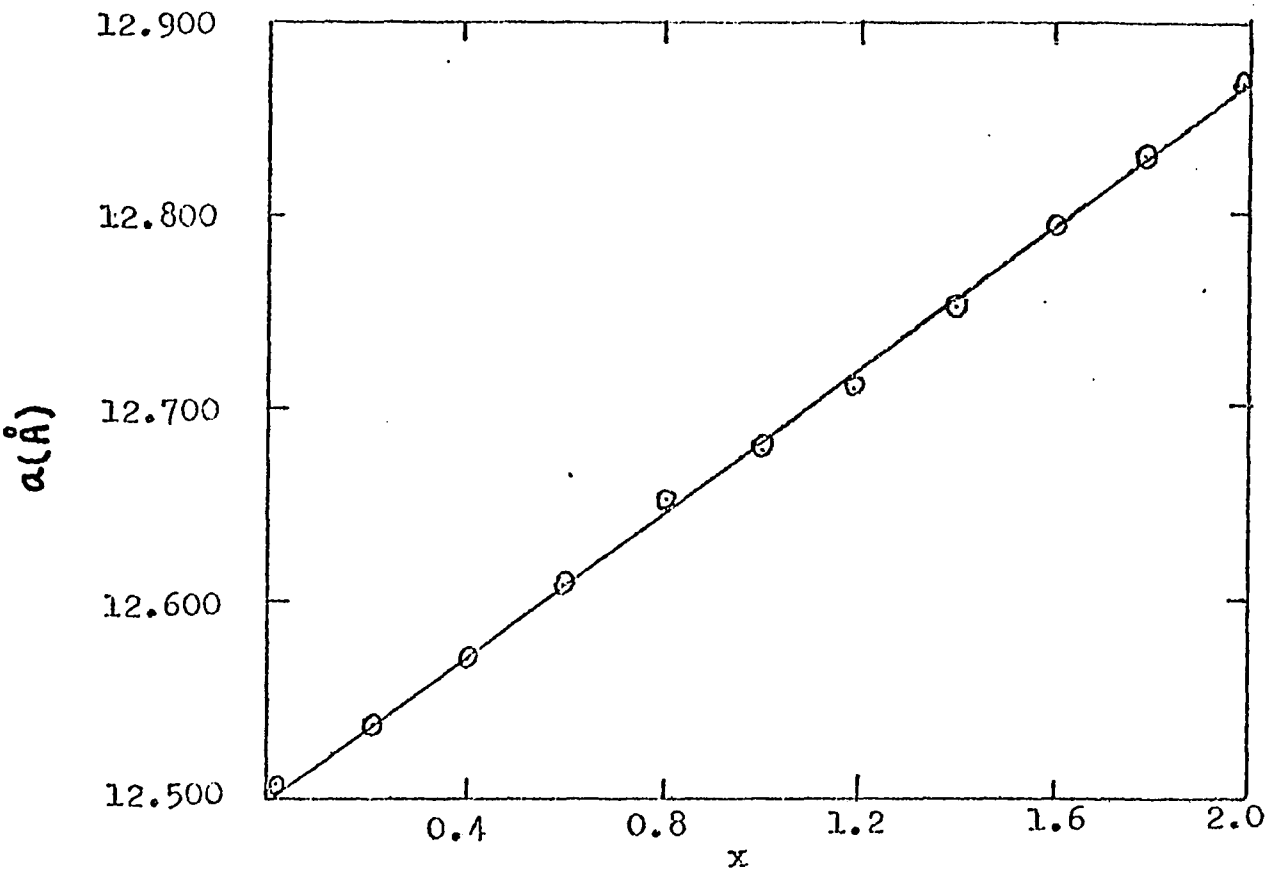

Fig. IV.6

Lattice constant versus x in $\{Pr_{2.7}Lu_{0.3}\}$ - $[Lu_xGa_{2-x}]$ $(Ga_3)O_{12}$ system.

Table IV.11 Calculated average Shannon-Prewitt 'IR' radii for the dodecahedral site containing Nd^{3+} or Pr^{3+} and minimum y-value amounts of small rare earths (R).

	Average Dodecahedral Site Radius (Å)	
R^{3+}	Nd^{3+} Compounds	Pr^{3+} Compounds
Er^{3+}	1.07_6	1.08_6
Tm^{3+}	1.09_4	1.00_0
Yb^{3+}	1.10_6	1.11_4
Lu^{3+}	1.11_0	1.12_3*

* This value is from the present work.

IV.5 $\{RE_{3-y}R_y\}[R_2](Ga_{3-z}Fe_z)O_{12}$ System

Attempts to determine the maximum value of z in order to have maximum amount of magnetic Fe^{3+} in tetrahedral sites were made.

IV.5.1 Results and discussion of the system $\{Nd_{2.8}R_{0.2}\}[R_2](Ga_{3-z}Fe_z)O_{12}$. In this system where R is Lu or Yb attempts to replace all the gallium by iron failed. The resulting compositions of this system are listed in Tables IV.12 and IV.13 and the lattice constants vs z values of system $\{Nd_{2.8}Yb_{0.2}\}[Yb_2](Ga_{3-z}Fe_z)O_{12}$ plotted in Fig. IV.7.

In this system the plot of lattice constants vs z-values is not a straight line. These results suggest that some of the iron (or gallium) goes to octahedral sites, thereby pushing some of the ytterbium or lutetium into dodecahedral

Table IV.12

$\{Nd_{2.8}Yb_{0.2}\}[Yb_2](Ga_{3-z}Fe_z)O_{12}$

z	Purity	a(Å)
0.0	Pure	12.842
0.2	Pure	12.833
0.4	Pure	12.843
0.6	Pure	12.852
0.8	Pure	12.862
1.2	Pure	12.881
1.3	Impure	-

Table IV.13

$\{Nd_{2.8}Lu_{0.2}\}[Lu_2](Ga_{3-z}Fe_z)O_{12}$

z	Purity	a(Å)
0.2	Pure	12.819
0.4	Pure	12.823
0.6	Pure	12.819
0.8	Slightly Impure	12.823
1.0	Impure	12.823
1.2	Impure	12.823

Fig.IV.7

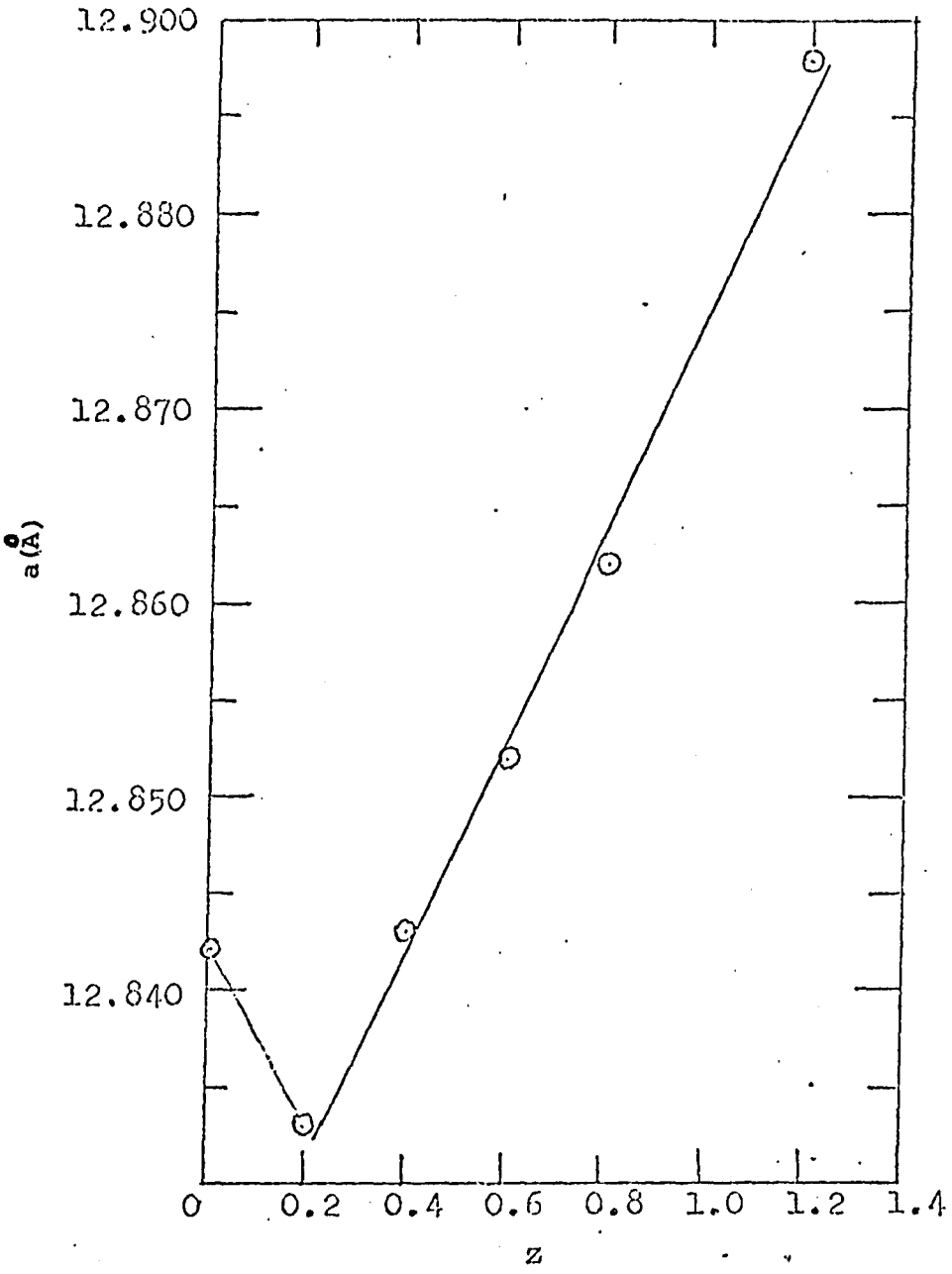

Lattice constant vs composition (in terms of z)

in $\{Nd_{2.8}Yb_{0.2}\}[Yb_2](Ga_{3-z}Fe_z)O_{12}$

site and forcing some of the Nd to exist in an additional phase. Although this second phase is not always detectable on x-ray film, it does effect on lattice constant.

IV.5.2 Results and discussion of the system $\{RE_3\}[Lu_2](Ga_{3-z}Fe_z)O_{12}$ system. In this system RE stands for Pr or Nd. Preparation of this system of garnets would permit study of pure rare earth Fe interactions (Lu^{3+} and Ga^{3+} are nonmagnetic ions).

Although attempts to replace some of the gallium by iron were successful (Tables IV.14 and IV.15), the plot of lattice constants vs z is not linear. The failure to get a straight line could be a result of a shift of the gallium or iron into octahedral sites or possibly some of the Lu going into dodecahedral sites.

Table IV.14

$\{Nd_3\}[Lu_2](Ga_{3-z}Fe_z)O_{12}$

z	Purity	a(Å)
0.0	Pure	12.881
0.2	Pure	12.845
0.4	Pure	12.874
0.6	Pure	12.852
0.8	Pure	12.855
1.0	Pure	12.861
1.2	Pure	12.870
1.3	Impure	-

Table IV.15

$\{Pr_3\}[Lu_2](Ga_{3-z}Fe_z)O_{12}$		
z	Purity	a(Å)
0.0	Pure	12.925
0.2	Pure	12.906
0.4	Pure	12.910
0.6	Pure	12.906
0.8	Pure	12.917
1.0	Pure	12.920
1.2	Pure	12.926
1.3	Slightly Impure	-

IV.6.1 $\{Sr_{3-x}La_x\}[Yb_2](Ge_{3-x}Fe_x)O_{12}$ and $\{Ca_{3-x}La_x\}[Yb_2](Ge_{3-x}Fe_x)O_{12}$ systems. In these systems the magnetic rare earth ion (Yb^{3+}) is on the octahedral site, the ferric ion is on the tetrahedral site, and the dodecahedral site contains nonmagnetic ions. These systems would make possible a study of octahedral-tetrahedral magnetic interactions. The results of Sr system is shown on Table IV.16. The magnetic properties of these compounds were not studied because it was not possible to put considerable amounts of iron in a tetrahedral site. The attempts to prepare the pure garnets of the second kind (Ca in dodecahedral sites) failed.

Table IV.16

$\{Sr_{3-x}La_x\}[Yb_2](Ge_{3-x}Fe_x)O_{12}$	
x	Purity
0.0	Pure
0.2	Pure
0.4	Pure
0.6	Slightly Impure
1.0	Impure
1.2	Impure
1.6	Impure
2.0	Impure
2.4	Impure
2.8	Impure
3.0	Impure

IV.7.1 Oxyfluoride garnets. Morell, Tanguy and Menil et al. (12) have studied oxyfluoride garnets of formula $Y_3Fe_{5-x}M_xO_{12-x}F_x$ and $Gd_3Fe_{5-x}M_xO_{12-x}F_x$ (M=3d transition elements by partial substitution of O^{2-} by F^- in $Y_3Fe_5O_{12}$ and $Gd_3Fe_5O_{12}$ oxides. The cationic charge compensation is obtained by replacing the Fe^{3+} ions by divalent ions such as Mn^{2+}, Co^{2+}, Ni^{2+}, Cu^{2+} or Zn^{2+}. Several other papers have been published which deal with such garnets (57, 58).

In the present work, attempts were made to prepare a few compounds of this type; the results of these attempts are listed in Table IV.17.

Table IV.17

Nominal Composition	Comment
$\{Sr_3\}[Lu_2](FeGe_2)O_{11}F$	Impure Garnet
$\{Ca_3\}[Lu_2](FeGe_2)O_{11}F$	Almost Pure
$\{Sr_3\}[Lu_2](Fe_3)O_9F_3$	Mostly Lu_2O_3 Lines
$\{Ca_3\}[Lu_2](Fe_3)O_9F_3$	Mostly Lu_2O_3 Lines
$\{Sr_3\}[Lu_2](Fe_{1.5}Ge_{1.5})O_{10.5}F_{1.5}$	Mostly Lu_2O_3 Lines
$\{Ca_3\}[Lu_2](Fe_{1.5}Ge_{1.5})O_{10.5}F_{1.5}$	Impure Garnet
$\{Ca_3\}[Lu_2](Fe_{0.6}Ge_{2.4})O_{11.4}F_{0.6}$	Slightly Impure
$\{Ca_3\}[Yb_2](Fe_{0.6}Ge_{2.4})O_{11.4}F_{0.6}$	Slightly Impure
$\{Ca_3\}[Ca_{0.25}Lu_{1.75}](FeGe_2)O_{10.25}F_{1.75}$	Slightly Impure
$\{Ca_3\}[Ca_{0.5}Lu_{1.5}](Fe_3)O_7F_5$	Not Garnet

V. APATITES

V.1 Introduction

The hexagonal apatite structure, typified by fluorapatite, $Ca_5(PO_4)_3F$, has been determined by Naray-Szabo (59).

There are six (PO_4) groups in the cell, 4 Ca ions on the trigonal axes surrounded prismatically by 6 O ions, and 6 Ca ions surrounded by an irregular polyhedron of a fluoride ion and 5 oxygens. Fluorides are at the corners of the reflection planes touching 3 Ca ions each.

In a great variety of compounds with this structure the Ca and P positions are occupied by various other cations and the F position by various other anions. As a general formula type one may write $A_5(BO_4)_3C$ (or $A_5B_3O_{12}C$). The unit cell contains two crystallographically inequivalent sites for the A ions (Ca in the case of fluoralatite). Four of the ten A ions have one type of coordination and the other six another type. The B ions (P in case of phosphate) are surrounded tetrahedrally.

If cations of proper size are chosen so that the total charge of 5 A's and 3 B's is 26+ (rather than 25+ as in $Ca_5(PO_4)_3F$), one can prepare a compound with oxide ions not only in the usual positions but in the C positions as well. This is a consequency of charge compensation; examples are $Ca_4La(PO_4)_3O$ and $CaY_4(SiO_4)_3O$ (or $A_5B_3O_{13}$) (60). Such compounds are called oxyapatites.

Another type of oxyapatite has a defect structure; an example is $Ca_5(PO_4)_3O_{0.5}\square_{0.5}$ (or $A_5B_3O_{12.5}$) where $\square$ represents a vacancy.

Such oxyapatities therefore have in each formula unit as written here 3 A II cations, 2 A I cations, 3 B cations, and 12.5 or 13 oxide ions. These ionic ratios (3:2:3:12.5-13) are therefore very close to those found in garnets (3:2:3:12).

In the present work attempts were made to prepare oxyapatites and fluorapatites with magnetic rare earth ions on A sites and a variety of ions on tetrahedral B sites and then to seek magnetic interactions as in the garnets.

V.2 Preparations

Preparations were made by solid state reaction (in some cases the preparations were repeated by the hydroxide method)* among various compounds (oxides, fluorides, carbonates, phosphates, etc.). Desired quantities of reactants were carefully weighed and intimately mixed by grinding with an agate mortar and pestle. Then the mixtures were heated for 24 hours at 1350°C in open crucibles (except that the crucible was covered when fluoride was involved) in a muffle furnace. After this, the samples were regrounded and reheated for 24 hours under the same conditions.

V.3 X-ray Diffraction Studies

X-ray patterns of prepared compounds were checked to see

*Desired quantities of reactants were mixed. This mixture was then added, with stirring, to ammonium hydroxide. The precipitate was filtered, washed with water, and dried at 100°C in an oven. Samples of the precipitates were heated for 6 hours at 1000°C in a muffle furnace. The remaining procedure was then as stated above.

whether they contained only lines belonging to the apatite structure. The patterns of $Ca_5(PO_4)_3F$ and $CaY_4(SiO_4)_3O$ were used for reference. The results are given in Tables V.1-V.7.

Table V.1

$Ca_5(PO_4)_3F$*

d Spacing	Intensity[a]
8.40	m
5.12	vw
4.05	w
3.90	w
3.45	s
3.18	m
3.08	m
2.81	vs
2.77	s
2.70	s
2.67	m
2.625	m
2.52	w
2.29	w
2.25	s^-
1.80	w^+
1.77	w^+
1.750	w^+
1.72	w^+
1.638	w
1.605	vw
1.47	w
1.425	w
1.400	w
1.275	w

*The result of this preparation agrees with the data given in literature (61).

[a] m stands for medium, vw for very weak, s for strong, and w for weak.

Table V.2

$RE_3M_2(XO_4)_3O$			
RE	M	X	Comment
Nd	Th	Fe	Mostly unreacted ThO_2
Sm			Unreacted ThO_2
Eu			Unreacted ThO_2
Gd			Unreacted ThO_2
Nd	Ce		Unreacted CeO_2
Sm			Unreacted CeO_2
Eu			Unreacted CeO_2
Gd			CeO_2 and Garnet phase
Tb			CeO_2 lines
Dy			CeO_2 lines
Ho			CeO_2 lines
Lu			CeO_2 lines
Er			CeO_2 lines
Yb			CeO_2 lines
Tm			CeO_2 lines
Nd	Th	Al	ThO_2 lines
Gd			ThO_2 lines
Er			ThO_2 lines
Nd	Ce		CeO_2 lines
Sm			CeO_2 lines
Tm			CeO_2 lines
Lu			CeO_2 lines
Nd	Th	Ga	ThO_2 lines
Gd			ThO_2 lines
Er			ThO_2 lines
Yb			ThO_2 lines
Nd	Ce		CeO_2 lines
Gd			CeO_2 lines
Yb	Ce		CeO_2 lines

Table V.3

$RE_5(M_3O_{11}F)O_{0.5}\square_{0.5}$

RE	M	Comment
Sm	Al	Perovskite phase
Ho		Mostly oxides lines
Yb		Mostly oxides lines
Sm	Fe	Mostly oxides lines
Dy		Mostly oxides lines
Lu		Mostly oxides lines
Nd	Ga	Mostly oxides lines
Gd		Mostly oxides lines
Er		Mostly oxides lines

Table V.4

$RE_5(M_3O_{11}F)F$

RE	M	Comment
Sm	Ga	Mostly oxides lines
Dy		Mostly oxides lines
Tm		Mostly oxides lines
Eu	Al	Contains perovskite phase
Lu		Mostly oxides lines
Dy		Mostly oxides lines
Nd	Fe	Mostly oxides lines
Gd		Mostly oxides lines
Yb		Mostly oxides lines

Table V.5

$RE_4X(MO_4)_3O_{0.5}\square_{0.5}$

RE	X	M	Comment
Nd	Ce	Ga	Mostly oxides lines
Gd			"
Er			"
Tm		Al	"
Dy			"
Nd			"
Lu	Th	Fe	"
Nd			"
Eu			"
Dy			"
Tm			"
Nd		Ga	"
Gd			"
Er			"
Dy		Al	"
Eu			"
Tm			"
Nd	Ce	Fe	"
Lu			"
Nd			Garnet phase
Gd			Mostly oxides lines
Ho			"
Tm			"
Eu			"

Table V.6

$RE_5(X_2YO_{12})F$

RE	X	Y	Comment
Nd	Fe	Si	Mostly oxides lines
Gd			"
Tm			"
Nd	Al	Ge	"
Dy			"
Lu			"
Nd	Fe	Ge	"
Gd			"
Yb			"
Gd	Ga	Ge	"
Er			"
Sm			"
Nd	Ga	Si	"
Dy			"
Lu			"
Sm	Al	Si	"
Ho			"
Yb			"

Table V.7

$RE_4X(MO_4)_3F$			
RE	X	M	Comment
Lu	Th	Fe	Mostly oxides lines
Eu			"
Er			"
Lu	Ce	Fe	"
Nd			"
Gd			"
Nd			"
Sm	Th	Al	"
Ho			"
Yb			"
Ho	Ce		"
Nd			"
Yb			"
Sm		Ga	"
Er			"
Dy			"
Nd	Th		"
Dy			"
Yb			"

V.4 Discussion

Substitution of P by Fe^{3+} and Ga^{3+} ions in apatite has not been reported. Fisher and McConnell (62) have claimed the substitution of some Ca and some P by Al^{3+} in $Ca_{10}(PO_4)_6F_2$ apatite but, they have also reported that the presence of Na is essential to the structure's stability.

In the present work attempts to replace some or all of P by Al^{3+}, Ga^{3+} or Fe^{3+} failed. The ionic radii for Fe^{3+}, Ga^{3+} and Al^{3+} (for CN=IV) according to Shannon-Prewitt (55) are 0.49Å, 0.47Å and 0.39Å respectively and all of them are larger than P^{5+} (0.17Å), Si^{4+} (0.26Å) V^{5+} (o.355Å or As^{5+} (0.335Å) which occupy the tetrahedral sites in reported apatites. This might suggest that these ions are too big for tetrahedral sites in the apatite structure although they are right for the tetrahedral site in the garnet structure.

Apatite with Si in tetrahedral sites have been reported (63) but, in the present work (Table V.6) attempts to prepare apatites with Si or Ge couples with iron, gallium or aluminum failed. It might again suggest that the presence of Al, Fe or Ga in tetrahedral sites prevents the formation of apatites. There is also the possibility of losing some F at high temperatures.

Probably Al^{3+}, Fe^{3+} and Ga^{3+} do not enter tetrahedral sites of apatite because tripositive ions on those sites yield a structure which is electrically unfavorable.

VI. MAGNETIC MEASUREMENTS

VI.1 Introduction

As mentioned earlier, in a pure rare earth iron garnet (MIG), (e.g., $\{Gd_3\}[Fe_2](Fe_3)O_{12}$) there is a very strong negative interaction between the Fe^{3+} ions on the a (octahedral) and d (tetrahedral) sites which induces all of the ions in each sublattice to enter into parallel alignment and the a and d sublattices into antiparallel alignment with one another. Since, per formula unit ($M_3Fe_5O_{12}$), there are two octahedral and three tetrahedral ferric ions, there will be a net magnetic moment equivalent to 1 ferric ion ($5\mu_B$) per formula unit from these two sublattices. If the rare earth ion is nonmagnetic (Y^{3+}, La^{3+}, Lu^{3+}), there is no further contribution. The other trivalent rare earths have their magnetic moments aligned by negative interactions with the ferric sublattices.

Geller et al., (7) have proposed that replacement of some of the octahedral Fe^{3+} ions by nonmagnetic ions such as Sc^{3+} ions as in $\{Gd_3\}[Sc_xFe_{2-x}](Fe_3)O_{12}$ causes random canting of the tetrahedral Fe^{3+} ions. Because the strong interactions of the Gd^{3+} ion moments are with those of the tetrahedral Fe^{3+} ion moments, this leads also to random canting of the Gd^{3+} ion moments thereby reducing the contribution of the dodecahedral sublattice to the net magnetic moment of garnet. Replacement of the tetrahedral Fe^{3+} by nonmagnetic ions as in $\{Gd_{3-x}Ca_x\}[Fe_2](Fe_{3-x}Si_x)O_{12}$ appears

to have no effect on the alignment of the Gd^{3+} ion moment.

In another paper Geller et al. have reported that the plot of $1/\chi_M$ vs T for the compound $\{GdCa_2\}[Zr_2](Fe_3)O_{12}$ is concave downward in the region of $30° \leq T \leq 50°K$ and this garnet appears to be weakly ferromagnetic, but the evidence presented for the weak ferromagnetism appears inadequate.

VI.2 Instrumentation

The single-phase preparations in Section IV.1.1 (with minimum value of y) were subjected to measurements at temperatures from 1.56 to 300°K.

These samples were measured with a null-coil pendulum magnetometer at a field strength of 15.3 kOe. in the laboratory of R. C. Sherwood of Bell Telephone Laboratories, Murray Hill, New Jersey.

The null-coil pendulum magnetometer was first used by C. A. Domenicali (64), in 1950 and an improved version of this instrument was made by Bozorth, Williams and Walsh (65) in 1956. R. C. Sherwood (66) has increased the sensitivity of this magnetometer by the use of semiconducting strain gages and a more stable bridge circuit.

The measurement of monents with the null-coil magnetometer is based on balancing the force which is exerted on a speciment when it is placed in homogeneous magnetic field. This force is balanced by means of a null-coil which produces a magnetic moment which is equal and opposite to that of the specimen.

The specimen is placed inside the null-coil which is in a field with a uniform gradient. The force on the system in the direction X of the gradient field is:

$$F_x = (m + iAN + m_c) \frac{\partial H}{\partial X}$$

where m is the magnetic moment of specimen, iAN (current x area x number of turns) is the moment of the coil due to the current, m_c is the moment induced by the field in the materials used in the coil and in that part of the pendulum which is in the field, and $\partial H/\partial X$ is the field gradient at the position of the specimen and coil. The correction term, m_c, is determined as a function of temperature by making a blank run on the empty coil to obtain values of i which make F=0 for selected applied fields.

If we designate the correction current i_c then

$$i_c AN + m_c = 0$$

and

$$F_x = [m + (i - i_c)\ AN]\ \partial H/\partial X;$$

consequently m can be measured as a function of i for various fields and temperatures.

A calibration constant (k) was calculated for the magnetometer by measuring the current needed to balance a saturated sphere of Johnson and Matthey spectroscopically-pure nickel. The moment of nickel σ_g, was taken as 54.39 emu/g at room temperature. The sphere weighed 0.1552 grams and the balancing current was 135.16 milliampere.

As mentioned above, the magnetic moment m, can be measured as a function of i for various fields and temperature:

$$m = ki.$$

Where k (a calibration constant) is constant. Therefore the equation for (magnetic moment/gram) will be:

σ_g = m/M, where M = weight of sample;

therefore $\sigma_g = ki/M$,

and $k = M\sigma_g/i$.

For Ni, $k = (54.39)(0.1552)(1/135.16)$

or $k = 0.0625$

for any sample $\sigma_g = (0.0625)i/\text{Weight of sample}$.

Therefore at each temperature was calculated by reading i and using the last formula. χ_g was calculated using the equations:

$\chi_g = \sigma_g/H$ H(magnetic field) = 15.3 k Oe.

and $\chi_M = (\sigma_g)(M.W)$ M.W = molecular weight.

The data obtained were put into the form of $1/\chi_M$ vs T, (Fig. VI.2-VI.4), σ_g vs H (Fig. VI.5-VI.8), and for $Sm_3[Sc_2](Fe_3)O_{12}$ and $\{Eu_3\}[Sc_2](Fe_3)O_{12}$ χ_M vs T was also plotted (Fig. VI.2). Molar Curie constants for paramagnetism were determined from the slopes of straight line portions of $1/\chi_M$ plots. The molar Curie constants (C_M) obtained from slopes of the straight line portions of the plots were given in Table VI.2 with those calculated from theoretical values using the magnetic moment values in Table VI.1. The number of Bohr magnetons shown in Table VI.3 were calculated from:

$$n_B = (M)(\sigma_g)/(5585).$$

Where n_B is the number of Bohr magnetons and M is the formula weight of the sample.

Data shown in Table VI.5 are the magnetic moments of rare earth garnets considering antiparallel and parallel alignment of spins on dodecahedral and tetrahedral sites. For Gd^{3+} the orbital angular moment L is zero. It is also assumed to be completely quenched in Fe^{3+}. The rare earth elements are divided at the point of half filled 4f shell into light (La-Eu) and heavy (Gd-Lu) groups. In these two groups, spin and orbital angular moments are couples yielding J equal to L-S for the light group and J = L+S for the heavy group.

For one of the compounds (to be discussed later) the magnetic measurement with high field was made by G. Hull in his laboratory at Bell Laboratories, Murray Hill, New Jersey. The method used in high field measurement was to extract the specimen from a series-connected coil and ballistic flux meter, the voltage being proportional to the moment. This instrument allows measurement of magnetic moment at zero field.

VI.3 Discussion of Results

The garnets $\{Nd_3\}[Sc_2](Fe_{2.6}Ga_{0.4})O_{12}$, $\{Nd_{2.3}Lu_{0.4}Sc_{0.3}\}[Sc_2](Fe_3)O_{12}$, $\{Nd_{2.3}Lu_{0.3}Sc_{0.4}\}[Sc_2](Fe_3)O_{12}$, $\{Nd_{2.4}Y_{0.4}Sc_{0.3}\}[Sc_2](Fe_3)O_{12}$, $\{Nd_{2.6}Gd_{0.1}Sc_{0.3}\}[Sc_2](Fe_3)O_{12}$, $\{Sm_3\}[Sc_2](Fe_3)O_{12}$, $\{Eu_3\}[Sc_2](Fe_3)O_{12}$, $\{Gd_{2.85}Sc_{0.15}\}[Sc_2](Fe_3)O_{12}$, $\{Tb_{2.75}Sc_{0.25}\}[Sc_2](Fe_3)O_{12}$, and $\{Dy_{2.7}Sc_{0.3}\}[Sc_2](Fe_3)O_{12}$

were subjected to measurements at temperatures from 4.2-300°K (field strength 15.3 kOe.). The data were put into the form of $1/\chi_M$ vs T plots and Curie constants, C_M, were determined from straight line portions (Table VI.2). In addition, measurements of magnetic moments of these garnets were made at temperatures lower than 2°K as a function of decreasing field and data were plotted as σ_g vs H.

$\{Gd_{2.85}Sc_{0.15}\}[Sc_2](Fe_3)O_{12}$ was also subjected to measurement at 4.2°K as a function of increasing field from 0-60.7 kOe. in order to seek saturation.*

The reason that two values of C_M (Table VI.2) for Nd compounds are reported herein is that in the $1/\chi_M$ vs T graphs for these compounds it is possible to find two straight lines (paramagnetic behavior) with different slopes.

For $\{Nd_3\}[Sc_2](Fe_{2.6}Ga_{0.4})O_{12}$ both values (10 and 13.3) of C_M are smaller than that of the theoretical value (16.2). These values indicate a trend of quenching of paramagnetic moment. In the other four Nd-Fe garnets the quenching appears to be effective at higher temperature and this effect fades out of the picture as the temperature drops (at lower temperatures the value of C_M shown in Table VI.2 is larger than the theoretical value for each of these compounds).

For five Nd-Fe garnets, antiferromagnetic ordering can be ruled out because in the case of antiferromagnetism,

*Measurement of all compounds with high field was not possible because the instrument was not available. Measurement of this sample was made by G. Hull in his laboratory at Bell Laboratories, Murray Hill, New Jersey. This sample was chosen because Gd^{3+} is a spin-only ion, which makes the interpretation simpler.

$1/\chi_M$ should decrease with decreasing temperature above the Néel point. In other words, the slope changes sign at the Néel temperature.

Ferrimagnetism or ferromagnetism is likely on the basis of these measurements because extrapolation of σ_g vs H curves do not show a σ_g value of zero at H=0 kOe. (this is the spontaneous magnetization explained earlier).

Table VI.5 shows the calculation of magnetic moments of these compounds considering ferromagnetic or ferrimagnetic behavior. Comparing spontaneous magnetization (Table VI.3) with these values does not give a quantitative explanation of any ferromagnetic or ferrimagnetic behavior. This is possibly because every sublattice (c and d) magnetization decreases with temperature but not necessarily at the same rate. The c-sublattice magnetization, which is not very strongly aligned, decreases most rapidly with temperature. If the c-sublattice (in the present case Nd) contribution is less than that of the d-sublattice (Fe), the ferric moment is dominant at all temperatures. The magnetization of the c-sublattice is the greatest at low temperatures and it will simply reduce the garnet magnetization at low temperature. As the temperature is raised, the rare earth contribution rapidly decreases. Eventually at high temperature the materials become paramagnetic.

At lower temperature the magnetic moments on two sites (c and d) start to cancel each other out, but in these materials the field is not strong enough to cause completely

antiparallel alignment of spins (i.e., canting occurs); that is why in these compounds magnetic saturation does not occur. In these materials (Nd-Fe garnets) the interaction is possibly the "uncompensated antiparallel spins: Néel type ferrimagnetism" shown in Fig. VI.1.

Fig. VI.2 shows the χ_M vs temperature curve for the compound $\{Sm_3\}[Sc_2](Fe_3)O_{12}$ for the field of 15.3 kOe. The outstanding feature of this curve is that χ_M increases as temperature decreases until T = 32.7°K, but at this point χ_M decreases with decreasing temperature. From this evidence and from zero spontaneous magnetization for this compound, it appears that Sm compound undergoes an antiferromagnetic behavior, but cooling with maximum field applied results in spontaneous magnetization. This possibly proves that Sm compound does not have antiferromagnetism behavior.

The interpretation of these results is that the Sm compound is ferrimagnetic at temperatures above 33°K. The Sm ion starts losing its moment at temperature around 33°K and because the iron's spins are already aligned at higher temperatures the Sm moment is the only major cause for decreasing χ_M at temperatures lower than 33°K. On cooling with field applied, the ionic moments of samarium remain more or less aligned and the result is spontaneous magnetization.

A plot of $1/\chi_M$ vs T (Fig. VI.2) for $\{Eu_3\}[Sc_2](Fe_3)O_{12}$ shows a considerable drop at T = 78.5°K. The curve at low temperature does not show any significant change of magnetization. This behavior means that $1/\chi_M$ is independent of

Fig.VI.1

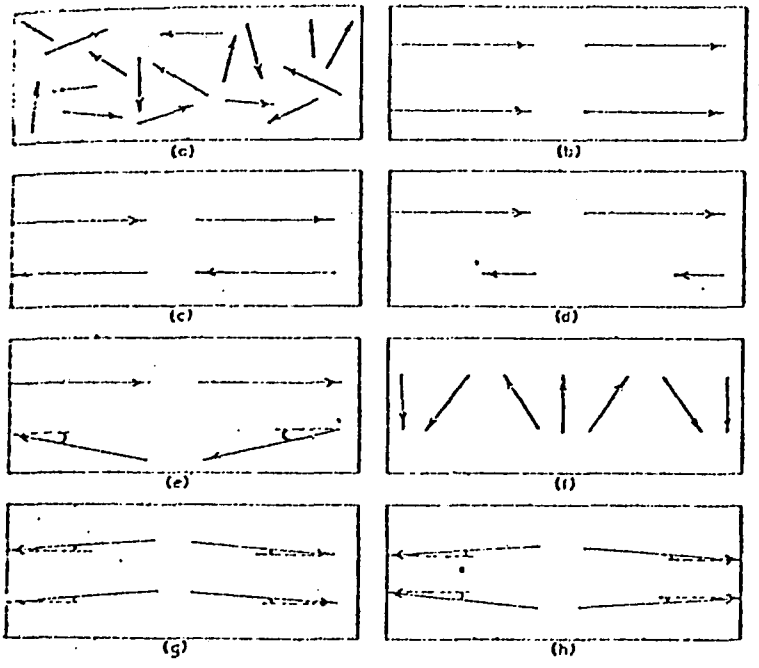

Schematic representation of spin arrangements: (Ref.67)

(a) disordered paramagnetic state
(b) parallel spins: ferromagnetism
(c) antiparallel spins: Néel type antiferromagnetism
(d) uncompensated antiparallel spins: Néel type ferrimagnetism
(e) triangular antiparallel spins: Yafet-Kittel type ferrimagnetism
(f) helical spiral structures: compensated antiferromagnetic or uncompensated ferrimagnetic
(g) canted spin Dzialoshinskii type weak ferromagnets
(h) canted spins compensated antiferromagnets; hidden canting.

temperature. The interpretation of this result is that the magnetic moment of iron does not change at low temperature and since the magnetic moment of Eu^{3+} is independent of temperature (68) the curve of $1/\chi_M$ vs T does not show any change (or significant change) at low temperature. The plot of σ_g vs H shows a spontaneous magnetization larger than zero; this is an indication of ferromagnetism or ferrimagnetism. This is possibly a ferrimagnetic behavior (with canting of moments), signaled by the slope changes in the curve $1/\chi_M$ vs T.

Plots of $1/\chi_M$ vs T for $\{Gd_{2.85}Sc_{0.15}\}[Sc_2](Fe_3)O_{12}$, $\{Tb_{2.75}Sc_{0.25}\}[Sc_2](Fe_3)O_{12}$ and $\{Dy_{2.7}Sc_{0.3}\}[Sc_2](Fe_3)O_{12}$ are shown in Fig. VI.4. These plots show magnetic ordering (change of slope) at temperatures around 90-50°K but not enough points were obtained in order to know the exact temperature of the slope change. The calculated value of the Curie constant, C_M, for these three compounds at higher temperature is close to the theoretical values (indication of paramagnetism.

Antiferromagnetism can be ruled out in these three garnets because $1/\chi_M$ does not go up at any temperature and it continues to go down as the temperature decreases. Ferromagnetism or ferrimagnetism cannot be rules out on the basis of these measurements because extrapolation of σ_g vs H curve does not show a spontaneous magnetization of zero for any of these three garnets.

The extrapolation of the straight portion of the $1/\chi_M$ vs T curve cuts the T axis below 0°K. This is an indication of ferrimagnetic behavior for Gd-Fe, Tb-Fe, and Dy-Fe garnets. Therefore the interpretation of the results for these three compounds is that the change of the slopes for $1/\chi_M$ vs T of these three compounds is due to ferrimagnetic ordering (with canting of ion moments).

For the Gd-Fe case measurement of magnetic moment in the field zero up to 60.7 kOe. is another indication of ferromagnetism or ferrimagnetism. The curve σ_g vs H (60.7 kOe.) at higher field starts to show the approach of saturation, which might occur at fields around 100 kOe.

Results would be more earily analyzed if magnetic saturation could be attained. The difficulty in reaching saturation is probably due to extreme canting of ion moments.

Table VI.1 Theoretical magnetic moment and individual gram-atom Curie constant (Ref. 69).

Ion	Theoretical* Magnetic Moment (μ)	$C_{(ind)}$[a]
Nd^{3+}	3.62	1.625
Sm^{3+}	0.84	0.087
Eu^{3+}	0.00	0.000
Gd^{3+}	7.94	7.816
Tb^{3+}	9.72	11.714
Dy^{3+}	10.65	14.063
Fe^{3+}	5.92	4.350

* The values for Eu^{3+}, Sm^{3+}, and Fe^{3+} taken from Ref. 70.

[a] For a paramagnetic ion the magnetic susceptibility is given by $\chi = C/T$ where C is the Curie constant. For any individual paramagnetic μ (magnetic moment) = $2.84(\chi T)^{1/2}$ and therefore for any individual atom $C_{(ind)} = (\mu/2.84)^2$.

Table VI.2 Experimental and calculated Curie constants (C_M) of rare earth iron-Sc garnets.

Compound	Experimental* (C_M)	C_M Calculated** From Theoretical Values
$\{Nd_3\}[Sc_2](Fe_{2.6}Ga_{0.4})O_{12}$	10.0 (13.3)	16.19
$\{Nd_{2.4}Y_{0.4}Sc_{0.2}\}[Sc_2](Fe_3)O_{12}$	10.9 (18.5)	16.95
$\{Nd_{2.3}Lu_{0.3}Sc_{0.4}\}[Sc_2](Fe_3)O_{12}$***	10.9 (25.6)	16.79
$\{Nd_{2.3}Lu_{0.4}Sc_{0.3}\}[Sc_2](Fe_3)O_{12}$***	10.9 (27.8)	16.79
$\{Nd_{2.6}Gd_{0.1}Sc_{0.3}\}[Sc_2](Fe_3)O_{12}$	11.9 (25.6)	18.06
$\{Sm_3\}[Sc_2](Fe_3)O_{12}$	10.4	13.32
$\{Eu_3\}[Sc_2](Fe_3)O_{12}$	14.7	13.05
$\{Gd_{2.85}Sc_{0.15}\}[Sc_2](Fe_3)O_{12}$	32.6	35.33
$\{Tb_{2.75}Sc_{0.25}\}[Sc_2](Fe_3)O_{12}$	47.1	45.26
$\{Dy_{2.7}Sc_{0.3}\}[Sc_2](Fe_3)O_{12}$	51.0	51.02

* These values were obtained from slopes of the straight portions of the plots $1/\chi_M$ vs T. For four of these compounds two values were obtained because two straight lines could be drawn in different regions.

** Using $C_{(ind)}$ shown in Table VI.1.

***For these two compounds as reported earlier (Ref.56) it is possible that some of Lu or all of it goes into the octahedral site but since Lu^{3+} and Sc^{3+} are both non-magnetic ions this change of site does not have any effect on magnetic behavior of these two garnets.

Table VI.3

Compound	Spontaneous Magnetization (BM)	
$\{Nd_3\}[Sc_2](Fe_{2.6}Ga_{0.4})O_{12}$	0.34	
$\{Nd_{2.4}Y_{0.4}Sc_{0.2}\}[Sc_2](Fe_3)O_{12}$	0.57	
$\{Nd_{2.3}Lu_{0.3}Sc_{0.4}\}[Sc_2](Fe_3)O_{12}$	0.67	
$\{Nd_{2.6}Gd_{0.1}Sc_{0.3}\}[Sc_2](Fe_3)O_{12}$	1.13	
$\{Nd_{2.3}Lu_{0.4}Sc_{0.3}\}[Sc_2](Fe_3)O_{12}$	0.93	
$\{Sm_3\}[Sc_2](Fe_3)O_{12}$	0.00	(0.56*)
$\{Eu_3\}[Sc_2](Fe_3)O_{12}$	0.08	
$\{Gd_{2.85}Sc_{0.15}\}[Sc_2](Fe_3)O_{12}$	0.60	(3.40**)
$\{Tb_{2.75}Sc_{0.25}\}[Sc_2](Fe_3)O_{12}$	0.80	
$\{Dy_{2.70}Sc_{0.30}\}[Sc_2](Fe_3)O_{12}$	0.65	

* from G. Hull data (Fig. VI.9)

** From the plot obtained for the case of cooling in field (Fig. VI.7) by extrapolating to H=0 and using (No. of BM) $= \frac{\sigma_g \times M}{5585}$

Table VI.4 J, L, S and g values for rare earth and iron ions (Ref. 70).

Ion	J	L	S	g
Nd^{3+}	9/2	6	3/2	8/11
Sm^{3+}	5/2	5	5/2	2/7
Eu^{3+}	0	3	3	-
Gd^{3+}	7/2	0	7/2	2
Tb^{3+}	6	3	3	3/2
Dy^{3+}	15/2	5	5/2	4/3
Fe^{3+}	5/2	0	5/2	2

Table VI.5

Compound	Theoretical Magnetic Moment of Garnet* (μ)			
	Spins Antiparallel	Spins Parallel	Ferro $\|gJ\|\{\} + \|gJ\|()$	Ferri $\|gJ\|\{\} - \|gJ\|()$
$\{Nd_{2.4}Y_{0.4}Sc_{0.2}\}[Sc_2](Fe_3)O_{12}$	22.85	7.15	22.85	7.15
$\{Nd_{2.3}Lu_{0.3}Sc_{0.4}\}[Sc_2](Fe_3)O_{12}$	22.53	7.47	22.53	7.47
$\{Nd_{2.6}Gd_{0.1}Sc_{0.3}\}[Sc_2](Fe_3)O_{12}$	22.81	7.19	22.81	7.19
$\{Nd_{2.3}Lu_{0.4}Sc_{0.3}\}[Sc_2](Fe_3)O_{12}$	22.53	7.47	22.53	7.47
$\{Nd_3\}[Sc_2](Fe_{2.6}Ga_{0.4})O_{12}$	22.82	3.18	22.81	3.18
$\{Sm_3\}[Sc_2](Fe_3)O_{12}$	17.15	12.85	17.15	12.85
$\{Eu_3\}[Sc_2](Fe_3)O_{12}$	15.00	15.00	15.00	15.00
$\{Gd_{2.85}Sc_{0.15}\}[Sc_2](Fe_3)O_{12}$	4.95	34.95	34.95	4.95
$\{Tb_{2.75}Sc_{0.25}\}[Sc_2](Fe_3)O_{12}$	9.76	39.76	39.76	9.76
$\{Dy_{2.7}Sc_{0.3}\}[Sc_2](Fe_3)O_{12}$	12.00	42.00	42.00	12.00

* The values are calculated from data in Table VI.4 μ (magnetic moment) for each ion = gJ = g (L±S)

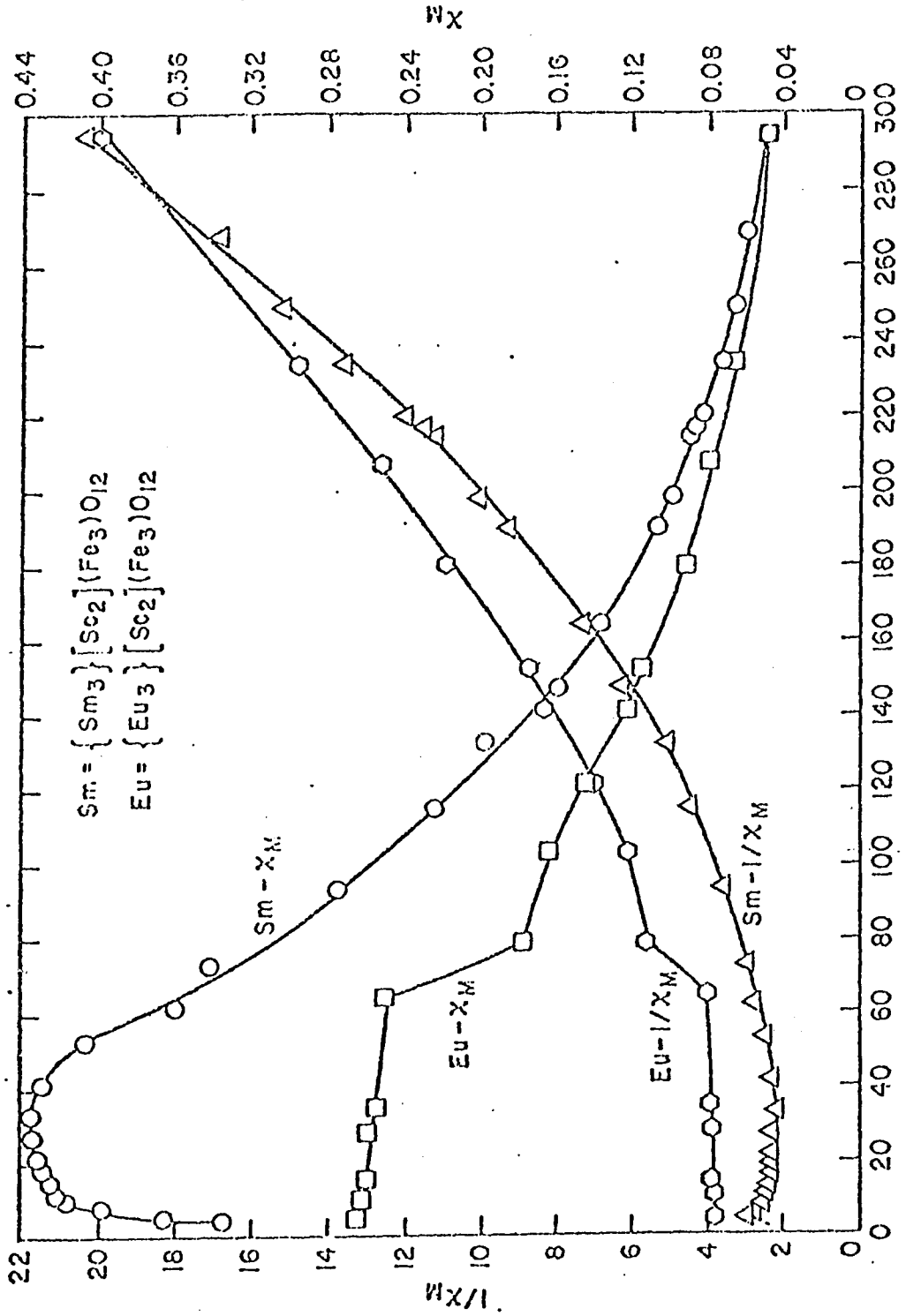

Fig. VI.2

Molar magnetic susceptibility and reciprocal molar magnetic susceptibility versus absolute temperature for $\{RE_3\}[Sc_2](Fe_3)O_{12}$, with RE = Sm and Eu.

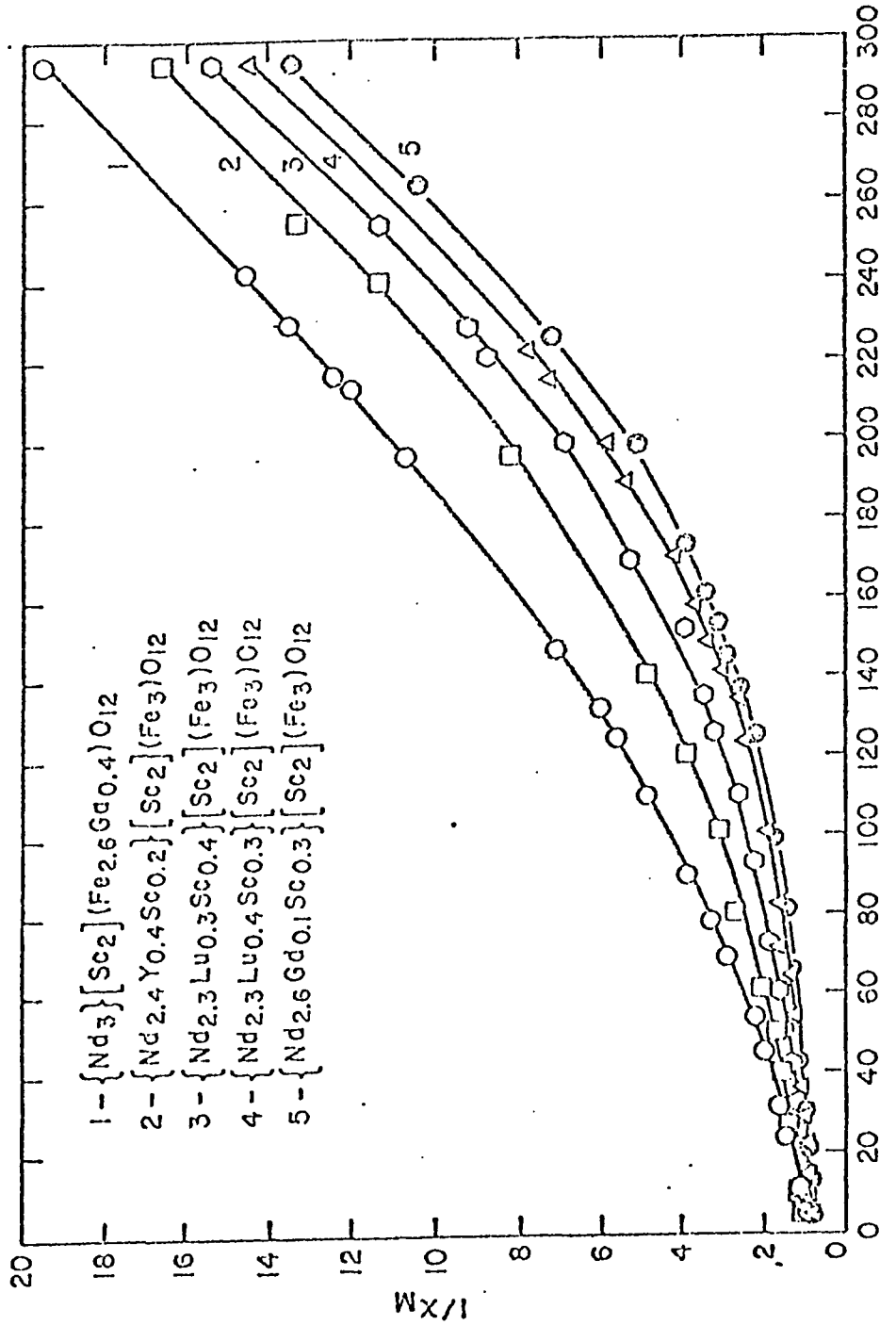

Fig. VI.3

Reciprocal molar magnetic susceptibility versus absolute temperature for Nd-Sc-Fe garnets.

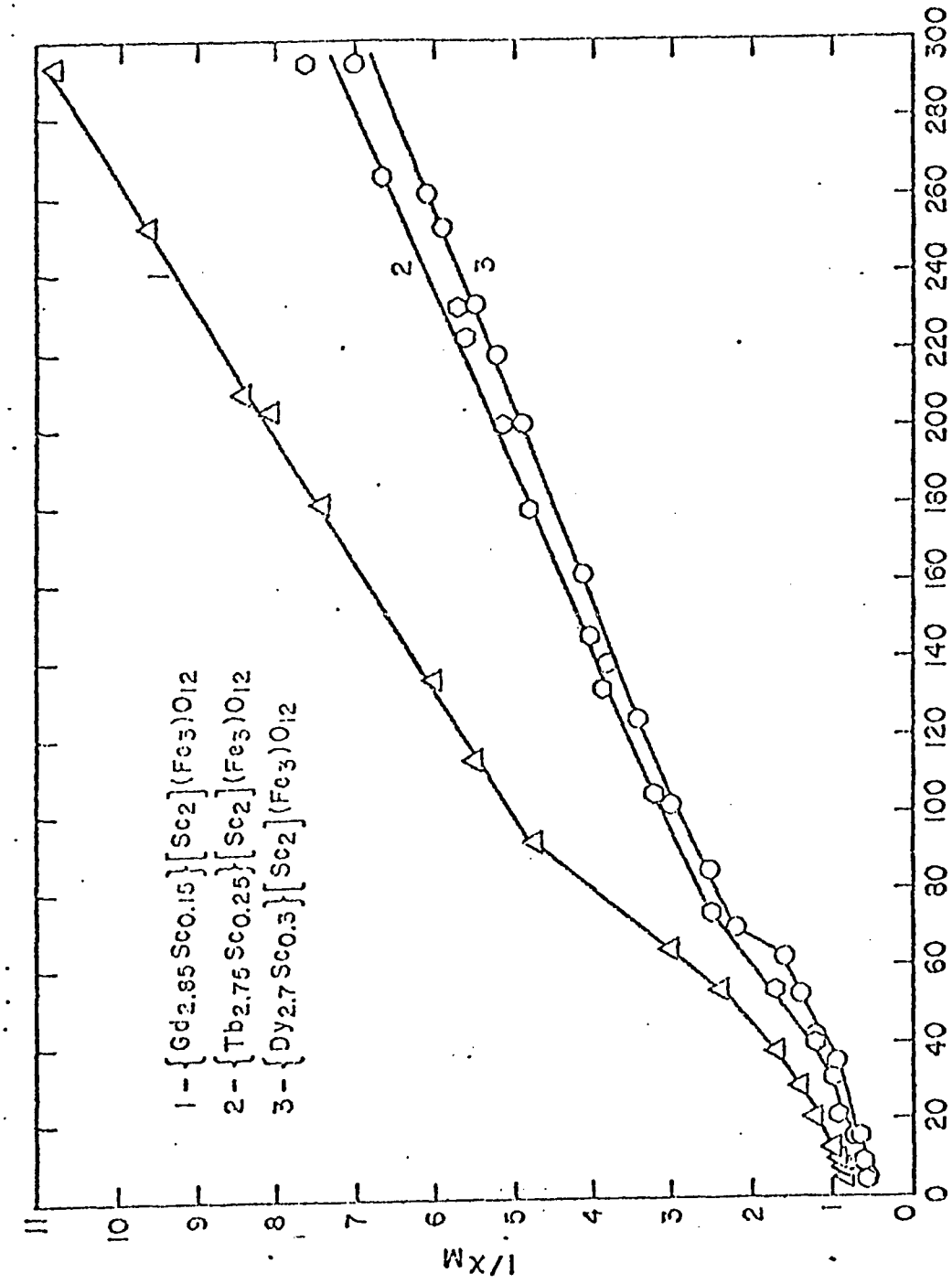

Reciprocal molar magnetic susceptibility versus absolute temperature for $\{RE_{3-y}Sc_y\}[Sc_2](Fe_3)O_{12}$, with RE = Gd, Tb, and Dy.

Fig. VI.4

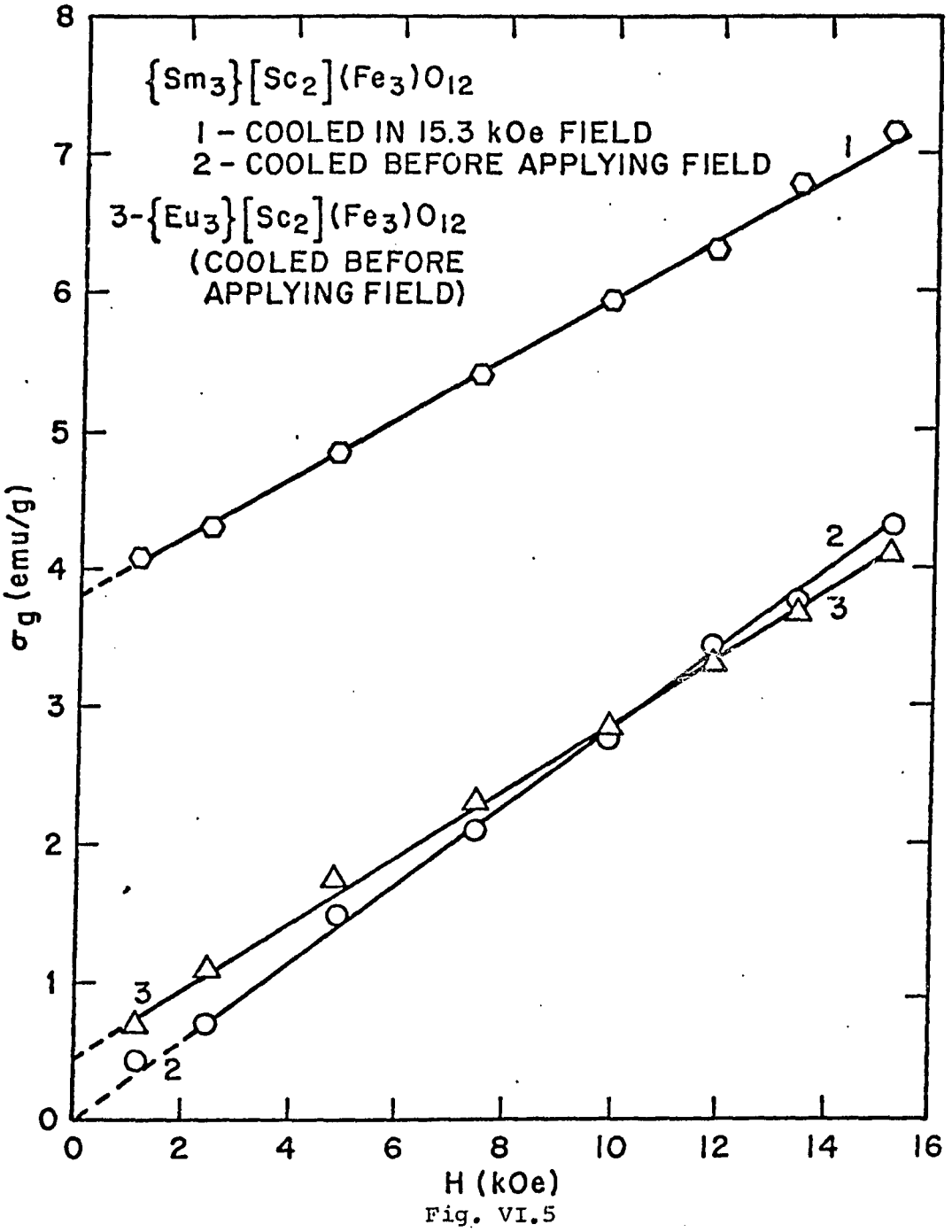

Fig. VI.5

Magnetization versus magnetic field for $\{RE_3\}[Sc_2](Fe_3)O_{12}$, with RE = Sm and Eu.

Fig. VI.6

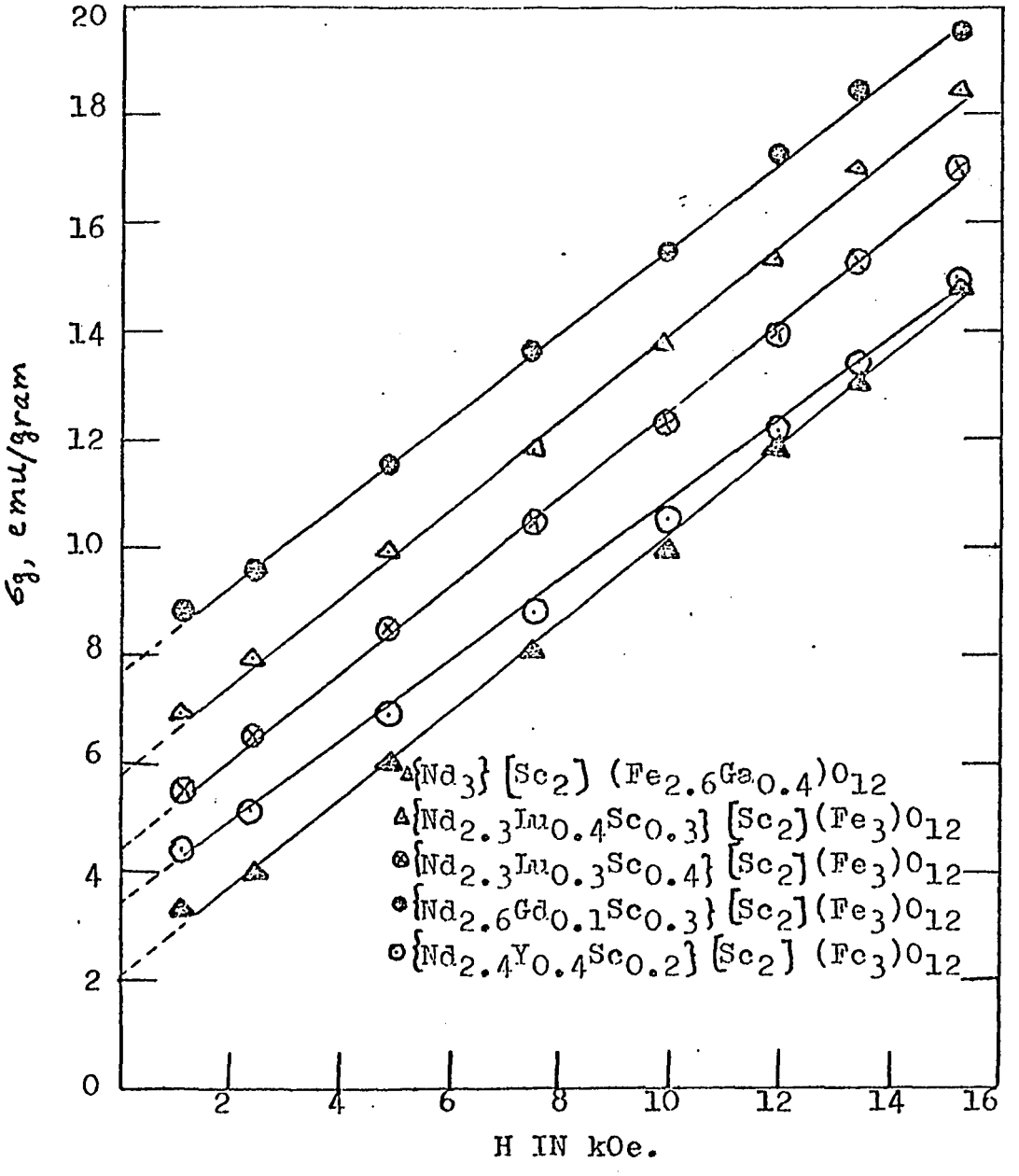

Magnetization versus magnetic field for $\{Nd_{3-(w+y)}M_wSc_y\}[Sc_2](Fe_{3-z}Ga_z)O_{12}$, with M=Y, Lu and Gd.

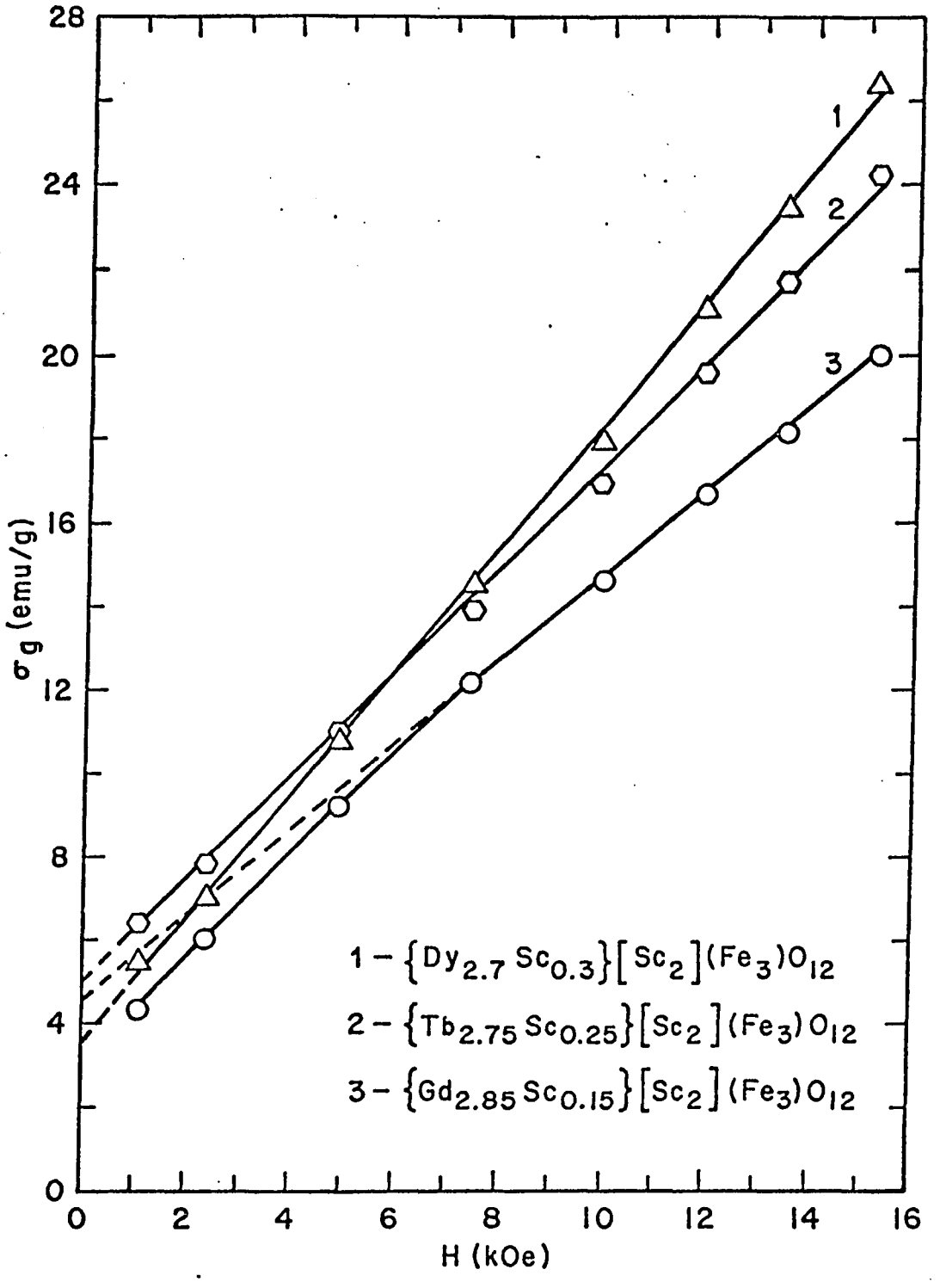

Fig. VI.7

Magnetization versus magnetic field for $\{RE_{3-y}Sc_y\}$-$[Sc_2](Fe_3)O_{12}$, with RE = Gd, Tb, and Dy.

Fig. VI.8

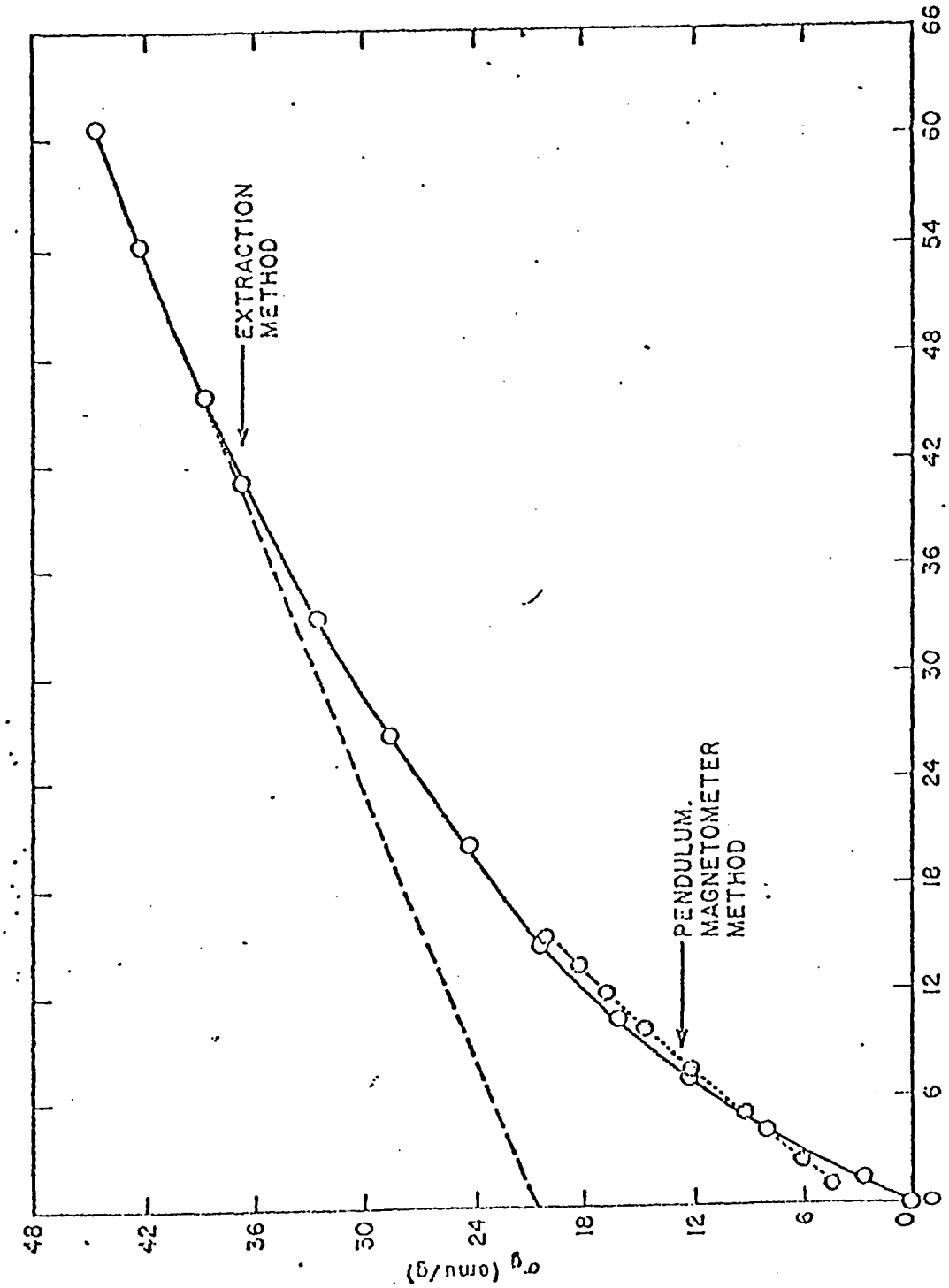

Magnetization versus magnetic field (two maximum values) for $\{Gd_{2.85}Sc_{0.15}\}[Sc_2](Fe_3)O_{12}$.

REFERENCES

(1) Menzer, G., Centralbl. Min. A 1925, 344-345; Z Kristallogr. 63, 157-158 (1926).

(2) Menzer, G., Z. Kristallogr. 69, 300-396 (1928).

(3) Geller, S., Z. Kristallogr. 125, 1-6 (1967).

(4) Geller, S., and M. A. Gilleo, J. Phys. Chem. Solids 3, 30-36 (1957).

(5) Novak, G. A., and G. V. Gibbs, The American Mineral. 56, 791-825 (1971).

(6) Gilleo, M. A., and S. Geller, Phys. Rev. 110, 73 (1958).

(7) Geller, S., H. J. Williams, R. C. Sherwood and G. P. Espinosa, J. Appl. Phys. 36, 88 (1965).

(8) Bertaut, F., Sur Quelqes Progres Recent Dans la Cristallographie des Spinelles, en Particulier des Ferrites J. Phys. Radium, 12, 252-255 (1951).

(9) Bertaut, F., and F. Forrat, C. R. Acad. Science Paris 243, 392-394 (1956).

(10) Geller, S., and M. A. Gilleo, Acta Crystallogr. 10, 239 (1957).

(11) Menzer, G., Die Kristallstruktur von Kryolithionit Z. Kristallogr. 75, 265-287 (1930).

(12) Morell, A., B. Tanguy, F. Menil and J. Portier J. Solid State Chem. 8, 253-259 (1930).

(13) Zemann, A., and J. Zemann, Acta Crystallogr. 14, 835-837 (1961).

(14) Coes, L., J. Amer. Ceram. Soc. 38, 298 (1955).

(15) Skinner, B. J., Amer. Mineral. 41, 428-436 (1956).

(16) Mill, B. V., Doki. Akad. Aauk (USSR) 156, 814-816 (1964).

(17) Strens, R. G., Amer. Mineral. 50, 260 (1965).

(18) Geller, S., and G. P. Espinosa, Not Published.

(19) Geller, S., and C. E. Miller, Amer. Mineral 44, 445-446 (1959).

REFERENCES (Continued)

(20) Swanson, H. E., and M. I. Cook, Standard X-ray Diffraction Powder Patterns NBS Circular 539, 10, 17-18 (1960).

(21) Swanson, H. E., M. I. Cook, E. H. Evans and T. Isaacs, NBS Circular 539, 9, 22-23 (1960).

(22) Geller, S., H. J. Williams, G. P. Espinosa and R. C. Sherwood, Bell System Tech. Jour. 43, 565-623 (1964).

(23) Mill, B. V., Zhur. Neorg Khim. 1533-1538 (1966).

(24) Geller, S., and C. E. Miller, Amer. Min. 44, 1115-1120 (1959).

(25) Geller, S., and C. E. Miller, Amer. Mineral. 44, 665-667 (1959).

(26) Kohn, J. A. and D. W. Eckart, Amer. Mineral. 47, 1422-1430 (1962).

(27) Gentile, A. L., and R. Roy, Amer. Mineral. 45, 701-711 (1960).

(28) Inoue, M., Phys. Rev. Letters, 11, 196 (1963).

(29) Yoder, H. S. and M. L. Keith, Amer. Mineral. 36, 519 (1951).

(30) Bertaut, F., and F. Forrat, C. R. Paris 242, 382-384 (1956).

(31) Coes, L., J. Amer. Ceram. Soc. 38, 298 (1955).

(32) Tauber, A., E. Banks and H. Kedesdy, J. Appl. Phys. 29, 385 (1958).

(33) Gilleo, M. A., and S. Geller, J. Phys. Chem. Solids 10, 187 (1959).

(34) Gilleo, M. A., and S. Geller, J. Appl. Phys. Supplement to Vol. 30, No. 4, 2975 (1959).

(35) Keith, M. L., and R. Roy, Amer. Mineral. 39, 1-23 (1954).

(36) Roth, R. S., J. Res. Nat. Bur. Stand. 58, 75-88 (1957).

(37) Schneider, S. J., R. S. Roth and J. L. Waring, J. Res. Nat. Bur. Stand. 65A, 354-374 (1961).

REFERENCES (Continued)

(38) Mill, B. V., Dokl. Akad. Nauk (USSR) 165, 555-558 (1965).

(39) Suchow, L., M. Kokta and V. J. Flynn, J. Solid State Chem. 2, 137-143 (1970).

(40) Suchow, L., and M. Kokta, J. Solid State Chem. 5, 329-333 (1972).

(41) Suchow, L., and M. Kokta, J. Solid State Chem. 5, 85-92 (1972).

(42) Suchow, L., and R. Mondegarian, J. Solid State Chem. 6, 553-560 (1973).

(43) "International Tables for X-Ray Crystallography," International Union of Crystallography, Kynoch Press, Birmingham, England (1952).

(44) Thomas, L. H., and K. Umeda, J. Chem. Phys. 26, 293 (1957).

(45) Card No. 12-768 of the Powder Diffraction File of the Joint Committee on Powder Diffraction Standards taken from U. S. National Bureau of Standards Monograph 25, Section 1, 1961.

(46) Euler, F., and J. A. Bruce, Acta Crystallogr. 19, 971 (1965).

(47) Tien, P. K., R. J. Martin, S. L. Blank, S. H. Wemple, and L. J. Varnerin, Appl. Phys. Lett. Vol. 21, No. 5, 1 September 1972.

(48) Geller, S., and M. A. Gilleo, Acta Crystallogr. 10, 239 (1957).

(49) Loriers, J., G. Villers, F. Clerc, and F. Lacour, C. R. Acad. SC Paris 268, 1553-1556 (1969).

(50) Mill, B. V., Izv. Akad. Nauk (USSR), Neorg. Mater. 5, 1839-41 (1969).

(51) Geller, S., H. J. Williams, G. P. Espinsoa, and R. C. Sherwood, Bell System Technical Journal 43, 565-623 (1964).

(52) Kokta, M., J. Solid State Chem. 8, 39-42 (1973).

(53) Kokta, M., Doctoral Dissertation, Newark College of Engineering, 1972.

REFERENCES (Continued)

(54) Gilleo, M. A. and S. Geller, J. Phys. Chem. Solids 10, 187, 1959.

(55) Shannon, R. D., and C. T. Prewitt, Acta Crystallogr., Sec. B 25, Part 5, 925-946 (1969) and R. D. Shannon and C. T. Prewitt, Acta Crystallogr., Sec. B 25, 1046-1048 (1970).

(56) Suchow, L., and M. Kokta, J. Crystal Growth 12, 257-258 (1972).

(57) Francillon, M., J. Loriers et G. Villers, C. R. Acad. So. 266, 1372 (1968).

(58) Tanguy, B., J. Portier, A. Morell, R. Olazcuaga, M. Francillon, R. Pauthenet et P. Hagenmuller, Mat. Res. Bull. Vol. 6, 63-68 (1971).

(59) St. Naray-Szaby, Szeged and P. T. Manchester, Z. Fur Krystallografie 75, 387-398 (1930).

(60) Steinbruegge, K. B., T. Henningsen, R. H. Hopkins, R. Mazelsky, N. T. Melamed, E. P. Riedel, and G. W. Roland, Appl. Optics 11, 999 (1972).

(61) Standard X-Ray Diffraction Powder Patterns NBS Monograph 25, Sec. 3, 25.

(62) Fisher, D. J., and D. McConnell, Science 164, 551-553 (1969).

(63) McConnell, D., "Apatite, Its Crystal Chemistry, Mineralogy, Utilization, and Geologic and Biologic Occurrences," Springer-Verlag, New York/Wien 1973.

(64) Domenicali, C. A., Rev. Sci. Inst. 21, 327 (1950).

(65) Bozorth, R. M., H. J. Williams, and D. E. Walsh, Phys. Rev. 103, 572 (1956).

(66) Sherwood, R. C., Private Communication, Bell Laboratories.

(67) Schieber, M. M., Experimental Magnetochemistry, North-Holland Publishing Company, Amsterdam, John Wiley & Sons, Inc., New York (1967).

(68) Morrish, A. H., The Physical Principles of Magnetism, John Wiley & Sons, Inc. New York (1965).

REFERENCES (Continued)

(69) Kern, S., and P. M. Raccah, J. Phys. Chem. Solids, Vol. 26, 1625-1628 (1965).

(70) Kauzmann, Walter, Quantum Chemistry, Academic Press, Inc., New York (1957).

VITA

Name ROSTAM MONDEGARIAN

Education: Iran Shahr High School
1959-1962, Yazd, Iran
Date of graduation: june 1962
University of Teheran
1962-1965, Teheran Iran
Date of graduation; June 1965
Bs in chemistry
Newark College of Engineering
1969-1972, Newark, New Jersey
Date of graduation: June 1972
MS in chemistry
Master Thesis:
STUDIES OF RARE EARTH COMPOUNDS
New Jersey Institute of Technology
1972-1976, Newark New Jersey
Doctor of Engineering Science In Chemical Engineering.

Doctoral project originated in the laboratory of Prof. L. Suchow at New Jersey Institute of Technology (previously Newark College of Engineering) from preliminary experiments of Prof. L. Suchow and M. Kokta in 1972. Some additional data were obtained in the laboratory of R. C. Sherwood and G. Hull of Bell Telephone Laboratories, Murray Hill, N.J., as mentioned in the text. This work has partly been supported by National science Foundation.